ANALYSIS OF NONLINEAR DYNAMICAL SYSTEMS: STUDIES IN CHAOS AND FRACTALS

A THESIS

SUBMITTED TO THE

UNIVERSITY OF POONA

FOR THE DEGREE OF

DOCTOR OF PHILOSOPHY

(IN CHEMISTRY)

BY

PARKASH BADOLA

M.Sc. (Biotechnology)

CHEMICAL ENGINEERING DIVISION

NATIONAL CHEMICAL LABORATORY

PUNE - 411 008

OCTOBER 1991

DEDICATED TO MY

PARENTS AND TEACHERS

Form - A

Certified that the work incorporated in the thesis **" Analysis of Nonlinear Dynamical Systems: Studies in Chaos and Fractals"** submitted by Parkash Badola was carried out by the candidate under my supervision. Such materials as has been obtained from other sources has been duly acknowledged in the thesis.

B. D. Kulkarni

Research Guide

ACKNOWLEDGEMENT

I am extremely grateful to my research advisor Dr. B. D. Kulkarni for guiding me in the research work presented in the thesis. It would not have been possible for me to complete this work had it not been for his valuable advice, encouragement and detailed scrutiny of the work at every stage. I shall always fondly cherish our professional association.

My sincere thanks are due to Dr. S. S. Tambe for his help rendered to me. I would also like to take this oppurtunity to sincerely thank Dr. Ravi Kumar for his suggestions during this research work. Also I express my heartfelt thanks to Mrs. Rajani Prasad for her crisp bits of advice while doing the work. Special mention goes to Dr. Satish Inamdar and Mr. Jayanta Bandhopadhyaya for their kind cooperation.

Dr. Ujwal Shinde, A. Chhatre, Archana Sharma and Murli Nair are also acknowledged for their kind cooperation.

I am greatly indebted to Dr. R. A. Mashelkar, Director of this Laboratory, for providing me all the facilities for doing research.

Finally, I thank the Council of Scientific and Industrial Research for the award of Fellowship during the tenure of this work.

(Parkash Badola)

C O N T E N T S

CHAPTER I

INTRODUCTION

1.1 Prologue

The order and highly collective behavior in open macroscopic systems as encountered in fields of biology, chemistry, sociology, astrophysics, computer science, economics etc. can be explained on the basis of laws of macroscopic physics and thermodynamics[1]. The observation that nonequilibrium can be a source of order has triggered explanation for collective behavior in many large scale dynamic systems which were once thought outside the scope of physics. Nonequilibrium constraints alongwith nonlinear dynamics switch on dissipative processes and thus set the stage for a variety of transition phenomena from bistability and sustained oscillations to chaos and spatial pattern formation. The term dissipative structures[2] i.e. structures resulting from dissipation rather than that from conservative molecular forces, include these phenomena. The onset and maintenance of order and self-organisation of the dissipative system is intimately linked with the stability properties, as these dissipative structures may only arise past an instability of the dynamical system. Two absolutely necessary ingredients in order to have instability are the non linearity of the kinetics and openness of the system. Dynamic systems with linear kinetics as also the isolated systems are always asymptotically stable no matter what the dimensionality of the system.

Despite the fact many of the complex systems may possess infinite degrees of freedom, they are still amenable to analysis, as a result of the developments made in the field of nonlinear analysis. Central to this analysis is the principle that in the parametric window corresponding to complex behavior a few collective degrees of freedom dominate the rest[1]. This research

work has been formulated and carried out with an objective to explain some of the features observed in such nonlinear systems. These new features illustrate newer dynamic patterns especially in the field of biology.

Chapter one briefly introduces the subject matter of the thesis. The literature on the various topics is reviewed in order to justify the work presented here.

Chapter two treats systems involving delayed feedback mechanisms[3]. Examples of systems described by either differential or difference equations are analysed. The effect of delayed feedback on logistic map shows that chaotic behaviour can be modulated with the introduction of delayed feedback in the system. Parameter α quantifies delayed feedback in the system. For intermediate values of α any kind of periodic or chaotic behaviour is suppressed. For higher values of α system exhibits period doubling route to chaos. In the second case study, example of cubic autocatalysis occurring in CSTR has been analysed. The results show presence of bursting phenomena. Examples of bursting are found in neural and respiratory systems in living organisms[4,5,6]. It has also been found to occur during epileptic seizures. Contrary to the belief that very complex models are needed to explain this kind of phenomena, it is observed in case of a very simple model of cubic autocatalysis with the effect of time delay introduced in the system equations. In the irreversible version of cubic autocatalysis in a CSTR, some fraction from the reactor output stream is recycled back into the cell after a delay. This introduces two new parameters in the system viz. time lag τ and fraction recycled λ. One major finding in this case study was that of bursting phenomena, which occurs when the slowly varying large amplitude oscillations in the CSTR are progressively disturbed by small parasitic oscillations. The time delay plays an important role

in the occurrence of bursting solutions. The appearance and disappearance of oscillatory bursting has been characterized with respect to fraction recycled and time delays. The study also includes the case where two recycle streams with different time delays are included in the system.

Chapter three involves studies in fractals. Fractals characterize irregular objects, which are envisaged as deviations from regular integer dimensional objects. These objects lack characteristic length scales[7]. They are characterized by their fractal dimension, a measure which assumes importance when the texture, roughness, dislocations and inhomogeneities assume a significant proportion such that the idea of a homogeneous object is no more valid. The aggregates which are formed due to irreversible flocculation of colloidal particles frequently exhibit self similarity of fractal structures. A simple stochastic model known as Diffusion Limited Aggregation (DLA) simulates the formation of such aggregation of particles[8]. A multi-step reaction has been studied on a DLA (Fractal) surface for its selectivity behavior using random walks. Periodic boundary conditions ensured that the simulated system is effectively part of an infinite system. Various methods are tried to decrease the computational time during the Monte-Carlo simulations. To specifically account for the percentage area occupied by active site and the fact that not all collisions will be energetically favored, various probabilities are assigned to each reaction step within physically realistic parameter ranges. The effects of varying probability of reaction steps and rate constants on selectivity behavior have been studied. Regions have been isolated where maxima and minima of selectivity occur.

In Chapter four the concept of chaotic dynamics is introduced. Chaotic phenomena is characterized by sensitivity to initial conditions and exponential divergence of nearby trajectories. Liapunov Exponents (L.E.) are the invariant properties of the underlying attractor which facilitate easy interpretation with respect to stability properties. The LE spectrum of a dynamical system is the signature of its dynamics. Chaotic dynamics is characterized by one positive LE. A hyperchaotic dynamical system[9] is characterized by at least two positive Liapunov exponents. In this chapter we analyze the glycolytic model in a living cell as proposed by Selkov[10]. Parameters corresponding to steady stable state, periodic, complex-periodic and chaotic dynamics have been identified. Results are interpreted in terms of information generation and loss in the system as it evolves.

In chapter five, extensive investigation has been carried out with a view to know what happens if an array of such cells start influencing each other dynamically. To begin with we start with a simple case of two cells. The idea that, two chaotic cells when coupled will synchronize, runs counter to our intuition. However, synchronization has been observed in coupled chaotic cells, together with emergence of periodicity for some other parameter values. In all the cases studied, fractal dimension of system attractor has been determined. Although the fractal dimensionality of the system attractor essentially refers to some static property, it is in fact related to dynamics of the system. A universal behavior of hyperchaotic-> periodic -> chaotic behavior has also been reported in coupled cells.

Chapter six analyses a class of autocatalytic network subject to mass constraints reported in the literature which has relevance in imperfect catalytic activity (as seen in the case of self-splicing RNAs, hypercycle theory). System behaviour has been characterized in terms of Liapunov exponents. Finally the significance of results obtained is discussed.

Chapter seven deals with difference equation schemes. These equations arise in many contexts in the biology, economics, hydrodynamics and population dynamics[11,12]. Mappings often provide the clues for understanding chaotic transition in higher dimensional systems. In contrast to 1-dimensional mappings, higher dimensional mappings offer the possibility of multiple stationarity. Starting from different basins of attraction the system may settle to different periodic or aperiodic orbits. Example of logistic map is taken for the analysis. In the three coupled cell configuration we chose the case wherein one cell can communicate with two others. This kind of unsymmetric coupling is reported in the literature for neural networks and spin glass models[13]. A new bifurcation transition of 4P--> 2P--> 4P that proceeds to chaos via period doubling has been observed. The effects of initial conditions demarcating the basins of attractors were analysed and show certain type of symmetry for this unsymmetrically coupled case.

Chapter eight finally concludes the thesis giving a concise summary of the results obtained and brings out the importance of the work.

1.2 References

1. H. Haken,(1983): *Synergetics - An Introduction, Non-equilibrium Phase Transitions and Self- Organization in Physics, Chemistry and Biology,* Springer, Berlin

2. G. Nicolis and I. Prigogine, 1977, *Self- Organization in Nonequilibrium Systems- From Dissipative Structures to Order through Fluctuation*, Wiley, New York.

3. Norman Mac Donald, Time Lags in Biological models, Lecture Notes in Biomathematics, Vol. 27, Springer- Verlag, New York 1978.

4. Joel Keizer and Paul Smolen, Proc. Natl. Acad. Sci. (USA) 88(1991) 3897.

5. B. Davies, L.S. Chattings and S. W. Edwards, J. Gen. Microbiol., 137 (1991) 705.

6. M. Onuzuka, S. Imai, H. Furuichi and S. Ozono, J. Neurobiol. 22(1991) 287.

7. B. B. Mandelbrot, *Fractals, Forms, Chance and Dimension*, Freeman, San Francisco, 1977.

8. T. A. Witten Jr. and L.M. Sander, Phys. Chem. Rev. 47 (1981) 1400.

9. O.E. Rossler, Phys. Lett. 71A (1979) 155.

10. Th. Schulmeister, Stud. Biophys. 72 (1978) 205.

11. R. M. May, Nature, 261 (1976) 459.

12. J. R. Beddington, C. A. Fru and J. H. Lawton, Nature 255 (1975) 58.

13. E. Domany and R. Meir, Europhys. Lett. 2(3) (1986) 175.

CHAPTER II

EFFECTS OF DELAYED FEEDBACK MECHANISMS ON MODEL SYSTEMS

This chapter studies systems involving delayed feedback mechanisms. The effect of delayed feedback on logistic map show that chaotic behaviour can be modulated with introduction of delayed feedback. For intermediate values of parameter α, which quantifies delayed feedback, any kind of periodic or chaotic behaviour is suppressed. In the second case, example of cubic autocatalysis taking place in CSTR is studied. Contrary to the belief that very complex models are needed to explain bursting phenomena, it is observed in case of a very simple model of cubic autocatalysis with the effect of time delay introduced in the system equations. In the irreversible version of cubic autocatalysis in a CSTR, some fraction from the reactor output stream is recycled back into the cell after a delay. Bursting occurs when the slowly varying large amplitude oscillations in the CSTR are progressively disturbed by small, parasitic oscillations. The time delay plays an important role in the occurring of bursting solutions. The study also includes the case where two recycle streams with different time delays are included in the system.

2.1 Introduction

The behaviour of dynamical systems is frequently described in the form of a set of differential or difference equations. The rate of change of variables usually depend only on their current values and a set of assigned parameters values. This implies that future behavior, can be obtained from the knowledge of the present state by integrating the equations. However, in many situations the future state depends on the past history, in addition to the current values of the variables. Such models then acquire the form of delay differential equations or the integro-differential equations[21,27]. In this chapter we shall study the effects of such delays for systems described by differential and/or difference equations.

2.2 Origin of time lags

In physiology, a number of systems involve a feedback signal that is transmitted as a nerve impulse, and the time of transition introduces a lag of the order of fraction of a second. The signal may also be transmitted by the circulation of a hormone, with rather longer lag. Discrete lag may often serve as an excellent approximation to such situations, but there is bound to be some spread of the lag around the mean value. Here the use of distributed lag may be seen as a way of allowing for a stochastic element in what is otherwise a deterministic model. Let us illustrate this by a simple example

Consider the equation of the following form

$$\frac{dx}{dt} = f(x, z) \tag{1}$$

setting $z = x$ gives an equation, in which the rate of change of x depends only on the current value,

$$\frac{dx}{dt} = f(x, x) = g(x) \tag{2}$$

To obtain a particular solution of the equation (2) for t > 0 one specifies the initial value x(0). Setting $z = x(t-T)$ introduces a discrete delay or discrete lag, and equation (1) becomes a delay-differential equation

$$\frac{dx}{dt} = f(x(t), x(t-T)) \tag{3}$$

To obtain a particular solution of equation (3) for t >0, one specifies values of x(t) over the range (-T to 0) of t. Setting

$$z = \int_{-\infty}^{t} x(\tau) G(t-\tau) d\tau \tag{4}$$

introduces a distributed lag, rendering equation (1) as an integro-differential equation.

$$\frac{dx}{dt} = f\left(x(t), \int_{-\infty}^{t} x(\tau) G(t-\tau) d\tau \right) \tag{5}$$

To obtain a particular solution of equation (5) for t > 0, one specifies values x(t) over all negative t. This is referred as memory function G(u). The memory function can be taken to be normalized

$$\int_{0}^{\infty} G(u) du = 1$$

The simple addition of time-lags in the governing system of equations transforms the finite dimensional system into one with infinite dimensions. The simple addition has a strong physical basis and a few examples illustrating the correspondence of lags to some physical features are discussed in the next sections.

2.3 Lags as an alternative to Age Structure

It is known that plants of certain species are pollinated by insects of one species only, and these obtain the nectar to feed their larvae from this one plant species only. It is natural, as a first approach to a model of this interaction, to work in terms of number of adult insects and mature (flower-bearing) plants. One then has to recognize that successful pollination is reflected in the number of new mature plants after some interval of time. An adequate supply of nectar is reflected in the emergence of new generation of adult insects from the larvae, again after an interval. A discrete time lag may be too crude an approximation and a memory function may be preferable. For making use of memory function, one has to work out detailed model in which the population dynamics of eggs, larvae, pre-adult instars and adults are specified. One may ofcource not have data complete enough for this to be possible. Thus, lags may serve as an alternative to age structure.

2.4 Lags as an alternative to Spatial Structure

Another reason for including a lag in a model may be that the real system has a spatial structure so that different stages in the process modelled take place in different regions. Then atleast one aspect of the spatial structure, the finite time for an intermediate component to cross from region to region, may be qualitatively modelled. Consider for example models of oscillatory biochemical processes in the cell[1,2]. These models are set up in terms of ordinary differential equations, treating the cell as spatially homogeneous, with all the reactions taking place uniformly throughout the cell. The reactions may have a natural source of lag, such as time taken to transcribe mRNA. But they may also involve transport from nucleus or membrane to cytoplasm. The finite time of transport could be included as a lag.

2.5 Lags and Stochastic Models

Let some process in a population model involve a discrete lag. For example each member of the population may hatch from an egg laid a time T_i which are distributed in a random manner, with a probability distribution P(T) which is peaked near the average lag model population $\overline{T}$. If this peak is sharp enough $\overline{T}$ may be used as the unique lag in a discrete lag

model of the population. Otherwise one could use a distributed lag model, the memory function being G(u) = P(u). Lewis[3] discusses various probability distributions that may be appropriate in this context. Corresponding to a given deterministic model for a variable x, it is possible to set up a linear stochastic model for the probability distribution P(x), which can be consistently expanded in the terms of appropriate small parameter. This small parameter can be a measure of the reciprocal of the system size, as discussed by van Kampen[4] or it may be a measure of the time scale of the fluctuations in x as compared with a natural time scale of the deterministic model, as discussed by White[5].

2.6 The Effects of Lag

It is expected that as the lag is made shorter, the stability or instability of the original steady state point should be recovered as in the original model. El'sgol'ts and Norkin[6] present a proof that this is the case, so long as lags are introduced only in the variables and not in the derivatives in the set of first order differential equations. In the usual terminology, this desirable result holds for retarded equations, but may not hold for neutral equations. Neutral equations have rarely been used in biological models although their use has been advocated by Lewis[7] in the context of population dynamics. The most typical effect of the lag is to destabilize an equilibrium point as the time lag is raised. The original bifurcation diagram is no more applicable, once delay is introduced in the system. Also the possibility of existence of strange attractors arises when the number of first order differential equations exceeds two. It is possible that a model may acquire such a solution when its dimensionality is raised from two by the incorporation of the linear chain, or when a discrete lag is incorporated[8].

2.7 Two Delays

In most situations the use of the simple one-delay equation is sufficient to describe the physics of the phenomena in question. There exists, however, certain situations in which a second delay must be added for a better approximation. Consider, for example, an optical cavity which is not completely filled by a nonlinear medium. In a normal completely filled

cavity the delay accounts the time taken by a photon to complete one round trip. In the unfilled cavity there are additional reflections at the interface of the nonlinear medium, with the result that a photon can take a number of different paths to arrive back at the same point. Each of these paths contributes an additional delay, whose effects must be added in the equations describing the system[9a,9b]. In the next sections we shall present the results showing the effects of time delays by considering model systems.

2.8 Case study 1

Difference equations provide a description for variety of problems[10]. Consider the case of simple logistic map

$$x_{n+1} = \lambda x_n (1 - x_n) \qquad (6)$$

As the value of parameter λ is varied the system exhibits variety of dynamic behaviour. Fig.1a depicts the period doubling bifurcation cascade culminating in chaos as the λ varies from 1 to 4. The effect of delay can be incorporated as

$$x_{n+1} = (1 - \alpha)\lambda x_n (1 - x_n) + \alpha \lambda x_{n-1} (1 - x_{n-1}) \qquad [(7)$$

To study the effect of delay in the equation in this model value of parameter α is varied from zero to one, keeping the value of parameter λ = 3.6. The resulting bifurcation diagram is depicted in the figure 1b. As can be seen by comparing both diagrams that for lower values of α, chaos which is present in the original model is still there, the system behaves as if the effect of delay term is negligible. It is followed by a region corresponding to intermediate values of α where the system exhibits single stable solution. In this region it can be clearly seen that any kind of oscillatory behaviour (periodic or aperiodic) is suppressed to steady stable solutions. For higher values of α system exhibits period doubling route to chaos.

2.9 Case study 2

2.9.1 Introduction

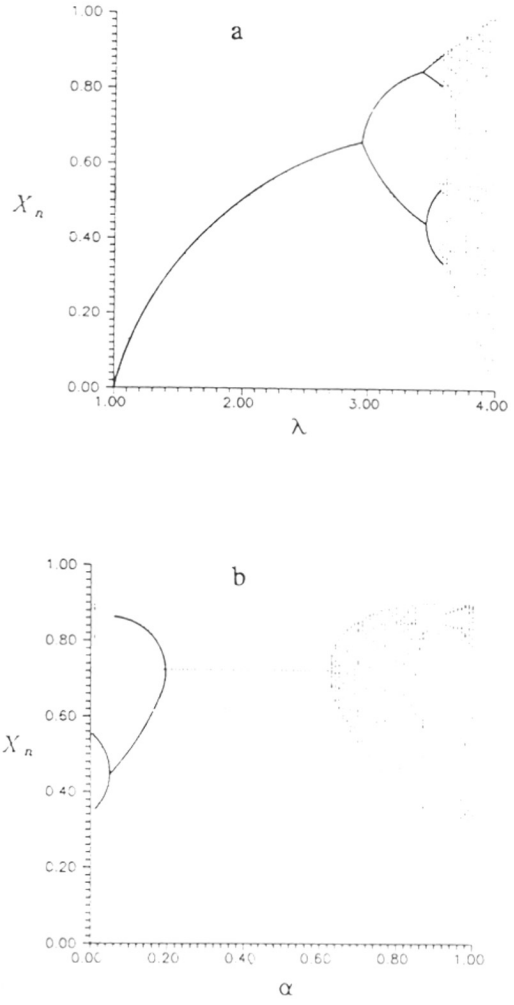

Figure 1a Bifurcation Sequence for X_n versus parameter λ for the Logistic Map. (b)Bifurcation sequence for X_n versus α for $\lambda = 3.6$.

Contrary to the general requirements that complex models are needed to explain the bursting solutions observed in several experimental systems, the present case study shows that bursting solutions are possible for a simple cubic autocatalytic reaction by invoking a mechanism of recycle and time delay.

Open nonequilibrium systems where there is a continuous supply of reactants and removal of products abound in nature as well as in designed processes. Systems operating under open conditions approach true stationary states which are different from the equilibrium states possible under closed conditions. Unlike in equilibrium processes, oscillatory conditions can be maintained indefinitely in these systems depending on the system mechanism and operating conditions. To study the basic features of systems operating under such conditions a number of theoretical and experimental studies on systems like the B-Z reaction[11], halide based oscillators[12], arsenite plus iodate reaction [13], enzyme systems and chain branching in gas phase reactions[14] especially under well stirred conditions have been carried out. An interesting oscillatory mode, namely, complex oscillations in the form of bursting or composed oscillations has been reported experimentally and has been a subject of extensive investigation[15].

The phenomenon of bursting is characterized by trains of one or more large-amplitude oscillations separated by trains of small amplitude oscillations which may be accompanied by periods of quiescence. For a chemically reacting system such as the Oregonator it has been conjectured[16] that a simple two or three composition variable model is unlikely to describe bursting solutions unless some mechanistic modifications are included in the system description. To simulate bursting solutions Boissonade[17] has thus suggested the introduction of a slowly changing parameter which could drive this model repeatedly between steady state and oscillatory behavior while other studies[18] allow the stoichiometric factor to be dependent upon the concentration of product.

The studies on coupled oscillators are also illuminating in this context where depending on the nature of oscillations and their coupling, the composed system can show a broad range of behavior[19]. The phenomenon of bursting in these systems occur as a result of interaction between two oscillating systems, each of which has a different frequency. It has been suggested that the slower oscillatory system switches the faster one alternately between its resting and its oscillatory mode[20].

The intention of the present case study is to show that the presence of delayed feedback in nonlinear processes is another route to produce bursting solutions typical of those experimentally observed. Delayed feedback models appear in various domains. Thus for instance time delay systems have been studied in biology[21], age-structured population models[22], nonlinear optoelectronics circuitry[23] and reacting systems[24]. The inherent effect of time delay has been noticed tacitly in cases of macromolecular reactions, where the time spent in diffusion of a macromolecule from the site where it has been produced to another site where it reacts again has to be accounted, as seen in the example of Goodwin's model of protein synthesis[25]. Rate processes with delayed feedback introduce a definite time lag which has a decisive influence on the system dynamics[26]. Dynamic studies with time lags in the process can be well described by differential-delay equations[27].

Skeleton reaction mechanisms describing many of the observed features with a minimum number of dependent variables have been preferred over more detailed mechanisms so as to strike at the causative factors responsible for the observations. To provide the feedback necessary for sustained oscillations in open reacting systems a frequently invoked concept is that of autocatalysis. Specifically a cubic rate form has been widely employed to describe chemical[28] and biochemical reactions[29] such as in the Hodgkin-Huxley equations and in its modified Bonhoefer van der Pol form. Also, to study the basic behavioral properties of nonequilibrium reacting systems a convenient structural model commonly employed allows the nonlinear process to take place in a continuous stirred tank reactor (CSTR). The advantage

of the CSTR model is that many physical situations wherein ingenious accounting for diffusion processes through coupling of CSTRs, external feedback mechanisms by allowing for recycle in the CSTR, effects of time delay processes by assuming time lags in the recycle stream etc., can be easily incorporated without increasing the rigor of obtaining solutions.

For the cubic autocatalysis in a CSTR (termed as autocatalator) the steady state and dynamic behavioral properties have been well characterized [30]. A parametric study with respect to varying residence time has classified the multiplicity and stability behavior in the form of bifurcation diagrams. Phenomena encountered include multistability, hysteresis, critical extinctions and ignitions, isolas and mushrooms. In our attempt to study the influence of delay processes on the above system we have modeled the autocatalator with a recycle stream, such that a part of the output from the reactor reenters it after a lapse of time. The incorporation of delay time in the model is in a broad sense related to studies of systems forced by periodic inputs[31] and also to cases wherein two chemical oscillators are coupled through the operation of a diffusion mechanism[32]. However, it may be pointed out that while the periodic input has its own autonomous existence, the present case is guided by system dynamics. Also, it differs from the coupled cell diffusion model due to lack of bidirectionality in mass transfer. The results presented here, however, focus their attention on the existence of bursting solutions in the autocatalator with recycle and a time delay mechanism operating. The experimental observation of bursting solutions in processes which are self-regulatory and the results obtained here on simulation do seem to indicate that invoking concepts of time delay may prove to be extremely fruitful in modeling system behavior.

2.9.2 The Model

The simplest form of the autocatalator with no reversible steps follows the mechanism:

$$A + 2B \xrightarrow{k_1} 3B$$

$$B \xrightarrow{k_2} C$$

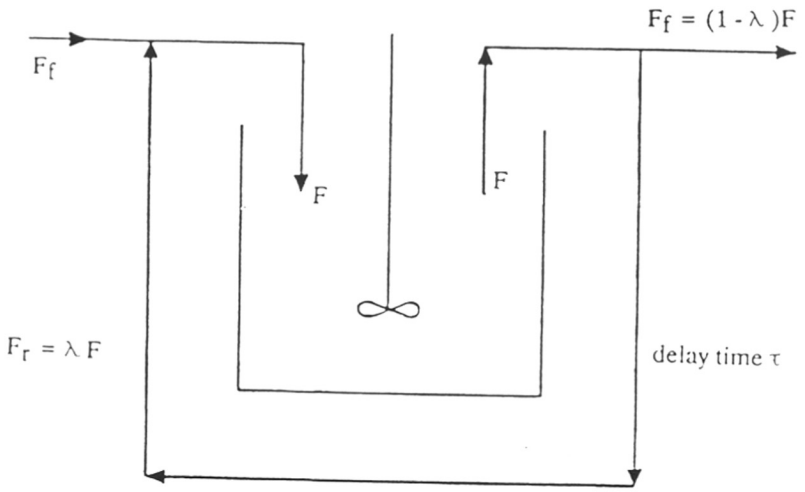

Figure 2 Schematic of CSTR with recycle and time delay

Figure 2 shows the schematic model of the CSTR with a recycle stream associated with a delay time τ units and where reaction corresponding to the above mechanism occurs. As seen the flow entering the reactor after a time lapse of τ units is composed of two contributions, namely, the continuous input from the external source and that of the recycle stream. If F_r is the flow rate in the recycle stream and F is that of the output stream then let us define the recycle ratio λ to be the fraction of total output stream recycled, i.e., $\lambda = F_r / F$. The relationships between the external input feed rate (F_f) and the recycle stream with the total reactor output is then given by

$$F_r = \lambda F \quad \text{and} \quad F_f = (1-\lambda)F \tag{8}$$

These relationships suggest that a reactor in the absence of a recycle stream has ($\lambda = 0$) while on the other hand ($\lambda = 1$) represents no input from the external feed ($F_f = 0$) and hence complete recycle. Let us assume that the total flow capable of entering the CSTR F is constant at all times. Therefore during the initial stages while time $t' < \tau$ units (when no contribution from the recycle stream exists due to the delay time) the external input is assumed to operate at a higher flow rate which decreases itself by an amount equal to F_r when $t' = \tau$.

For the CSTR of volume V, with a_f and b_f being the concentrations of species A and B in the external input the two coupled differential delay equations describing the system are,

$$V\frac{da}{dt'} = (1-\lambda)Fa_f + \lambda F a_{|t'-\tau} - Fa - k_1 a b^2 V \tag{9}$$

$$V\frac{db}{dt'} = (1-\lambda)Fb_f + \lambda F b_{|t'-\tau} - Fb + (k_1 a b^2 - k_2 b)V \tag{10}$$

$$a_{|t'-\tau} = 0, \quad \text{and} \quad b_{|t'-\tau} = 0, \quad \text{for} \quad t' < \tau \tag{11}$$

In the above equations the second term in the r.h.s. portrays the flow due to recycle with concentrations $a_{t'-\tau}$ and $b_{t'-\tau}$ as a function of the output from the CSTR at $t-\tau$ time units earlier. Equation (11) stipulates the condition that this second term for $t' < \tau$ does not contribute to the dynamics of the process. By defining the following dimensionless groups

$$x = \frac{(a_f - a)}{a_f}, \quad y = \frac{b}{a_f}, \quad t = k_1 a_f^2 t'$$

$$\alpha_1 = \frac{k_2}{(k_1 a_f^2)}, \quad \beta_1 = \frac{b_o}{a_f}, \quad \gamma = \frac{F}{V k_1} a_f^2 \tag{12}$$

Eqs. (9) and (10) can be rewritten in the following form,

$$\frac{dx}{dt} = \lambda \gamma x|_{t-\tau} - \gamma x + (1-x) y^2 \tag{13}$$

$$\frac{dy}{dt} = (1-\lambda)\beta_1 \gamma - \gamma y + \lambda \gamma y_{|_{t-\tau}} + (1-x) y^2 - \alpha_1 y \tag{14}$$

From Eqs. (13) and (14) it is possible to relate in a simple fashion the solution behavior of the system in the absence of recycle ($\lambda = 0$), with that of the CSTR operating with recycle (λ = finite) but without delay time ($\tau = 0$), by utilizing $x_{|_{t-0}} = x$ and $y_{|_{t-0}} = y$. Thus if γ_{wr} represents the dimensionless group for a case without recycle, then we have the relationship

$$\gamma = \gamma_{wr}/(1-\lambda), \quad \text{for} \quad \tau = 0 \tag{15}$$

with the remaining dimensionless groups α_1, β_1 retaining original values. The advantage of such a relation is that the earlier results which characterize the behavior of the autocatalator[30] in its parameter space can be *a-priori* utilized in the analysis of the dynamics of the autocatalator with recycle and base cases for studies easily chosen.

2.9.3 Results and Discussion

The results of solving the time delay model showed the existence of bursting solutions in an identified parameter range. The solution behavior indicated a sequential transition from

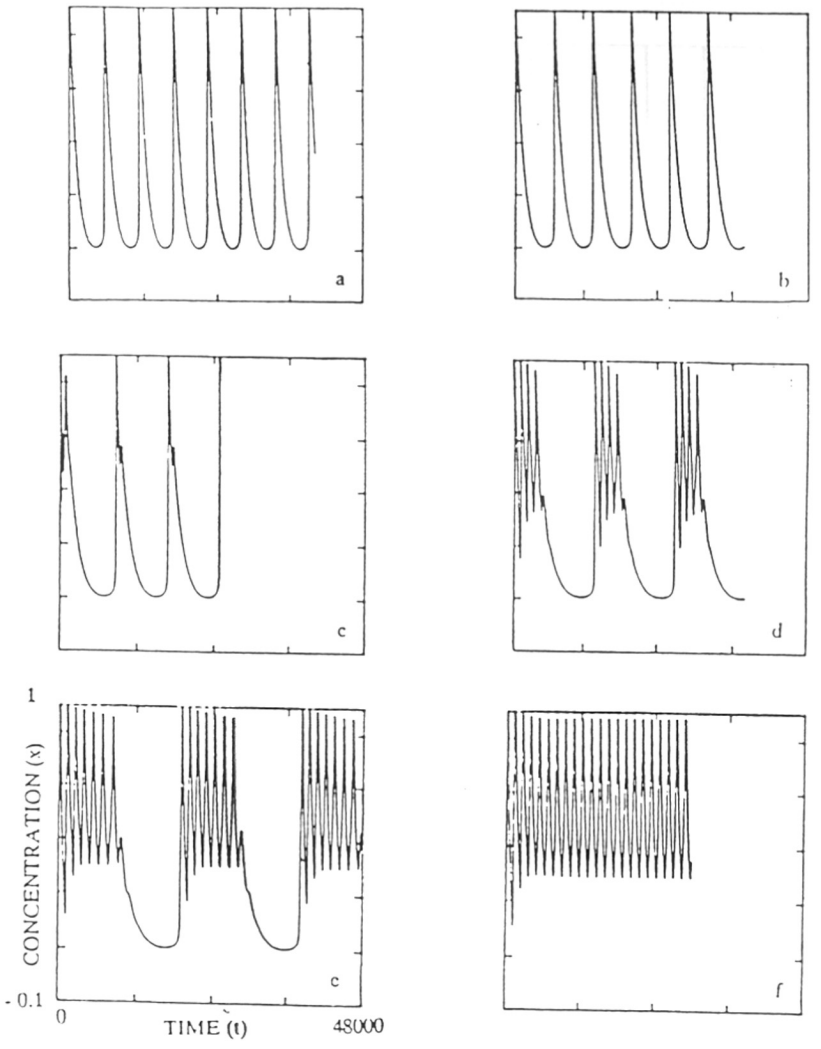

Figure 3 Dimensionless concentration time plots (*a-f*) for different values of delay time (τ = 0, 250, 500, 1000, 1080, 1100) respectively with constant recycle ratio (λ = 0.5)

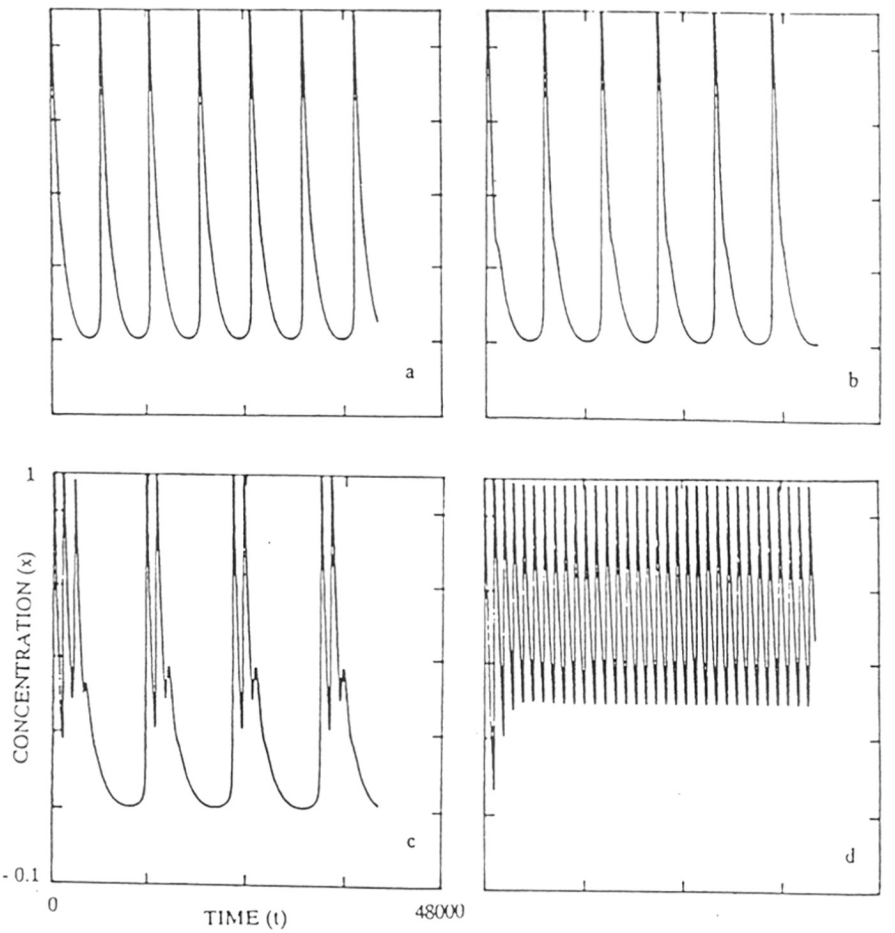

Figure 4 Dimensionless concentration time plots (*a-d*) for different values of recycle ratio (λ = 0.1, 0.2, 0.4, 0.6) respectively with constant delay time (τ = 1080).

periodic to bursting and back to periodic for a systematic variation in the key parameters, namely, the delay time τ and recycle ratio λ. The solutions to the delay-differential equations [Eqs. (13) and (14)] were obtained using a Semi-implicit Runge Kutta method incorporating a variable step size algorithm. To evaluate the appropriate values of $x|_{t-\tau}$ and $y|_{t-\tau}$ a cubic spline interpolation routine was built into the main algorithm. This interpolation routine returned the exact values of $x|_{t-\tau}$ and $y|_{t-\tau}$ from the past values of x and y as and when required by the main routine. The numerically integrated values are accurate to the order of 10^{-7}.

The earlier bifurcation study[30a] has shown that with parameter values corresponding to $\alpha_1 = 0.0166$, $\beta_1 = 0.11$ $\gamma_{wr} = 0.0008658$, and in the absence of recycle the system has three unstable steady states classified as an unstable node, saddle point and unstable focus. On dynamically integrating the system equations, relaxation oscillations were observed since all the steady state solutions are unstable. On choosing a recycle ratio of λ as 0.5, the relaxation oscillations were identically reproduced on adjusting the value of γ to 0.0017316, obtained *via* Eq. (15). Figure (3a) shows the dimensionless concentration profile x with time and forms the base case for the delay time $\tau = 0$. Retaining the value of $\lambda = 0.5$, the nature of the profiles on increasing the delay time τ from 250 to 1100 are shown in Figures 3b to 3f. It is seen that for $\tau = 250$ (Fig. 3b) the system continues to perform single peak relaxation oscillations. However, on increasing τ to 500 each cycle has an additional peak showing the onset of a bursting solution (Fig. 3c). The relaxation phase of the solution follows the appearance of the peaks. The number of peaks appearing rises for higher $\tau = 1000$ (Fig. 3d) and for $\tau = 1080$ (Fig. 3e), the total number of peaks observed was eight. The profiles seen are typical of bursting solutions where the system exhibits two types of modes -- a high amplitude oscillatory mode and a quiescent phase with regular repetition of the complex pattern. At still higher values of $\tau = 1100$ (Fig. 3f) the bursting nature is quenched and the system performs harmonic oscillations, albeit with a higher frequency than the relaxation oscillations observed in the

absence of time delay (Fig. 3a).

To further establish that the bursting nature of the solutions are induced by the combined presence of time delay and recycle for the autocatalator the recycle ratio was varied from $\lambda = 0.1$ to $\lambda = 0.6$, for $\tau = 1080$ corresponding to Fig. 3e in the previous study. The results for $\lambda = 0.1$, $\lambda = 0.2$, $\lambda = 0.4$ and $\lambda = 0.6$ are shown in Figs. 4a to 4d respectively. We again note that the system undergoes transitions from single peak periodic to bursting and back to a higher frequency oscillatory mode.

A simple model of a cubic autocatalytic reaction in a continuous stirred tank reactor in the presence of recycle and time delay has been investigated to show the existence of bursting solutions in certain regions of parameter space. The models hitherto known to exhibit this feature are usually more complex.

2.10 Two delays

In the equation 9,10,11 the effect of second delay with recycle can be easily incorporated by taking into consideration two recycle streams with recycle ratio λ_1, λ_2 with corresponding time delays τ_1, τ_2 where $(\tau_1 < \tau_2)$. The equations become

$$V\frac{da}{dt'} = (1-\lambda)Fa_f + \lambda_1 Fa_{|_{t'-\tau_1}} + \lambda_2 Fa_{t'-\tau_2} - Fa - k_1 ab^2 V \qquad (16)$$

$$V\frac{db}{dt'} = (1-\lambda)Fb_f + \lambda_1 Fb_{|_{t'-\tau_1}} + \lambda_2 b_{t'-\tau_2} - Fb + (k_1 ab^2 - k_2 b)V \qquad (17)$$

$$a_{|_{t'-\tau_1}} = 0, \quad \text{and} \quad b_{|_{t'-\tau_1}} = 0, \quad \text{for} \quad t' < \tau_1 \qquad (18)$$

$$\lambda = \lambda_1 + \lambda_2$$

$$a_{|_{t'-\tau_2}} = 0, \quad \text{and} \quad b_{|_{t'-\tau_2}} = 0, \quad \text{for} \quad t' < \tau_2 \qquad (19)$$

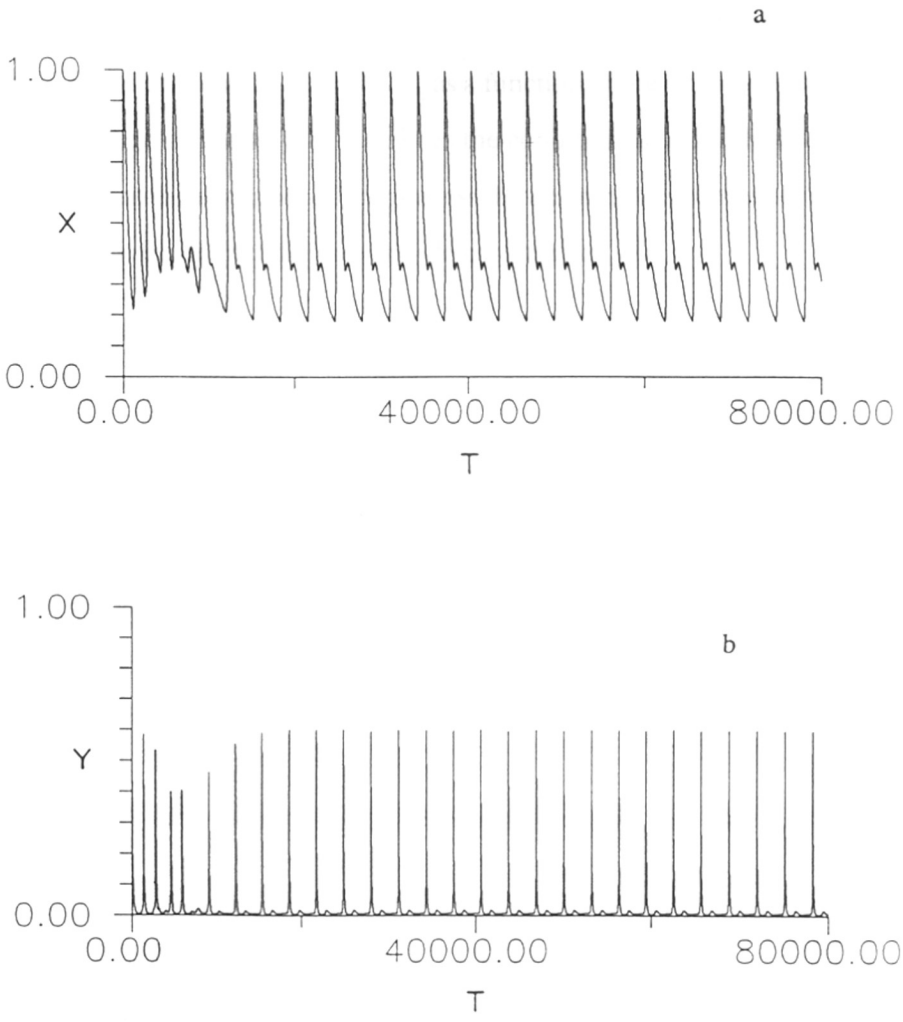

Figure 5a Concentration profiles of x incorporating the effects of second delayed feedback corresponding to $\tau_1 = 1080, \tau_2 = 2000$
$\lambda_1 = .5, \lambda_2 = .5$(b) concentration profile for y

In the above equations the second term in the r.h.s. portrays the flow due to recycle with concentrations $a_{t'-\tau_1}$ and $b_{t'-\tau_1}$ as a function of the output from the CSTR at $t-\tau_1$ time units earlier. Equation (18) stipulates the condition that this second term for $t' < \tau_1$ does not contribute to the dynamics of the process. Similarly the third term in the r.h.s. portrays the flow due to recycle with concentrations $a_{t'-\tau_2}$ and $b_{t'-\tau_2}$ as a function of the output from the CSTR at $t-\tau_2$ time units earlier. Equation (18) stipulates the condition that this third term for $t' < \tau_2$ does not contribute to the dynamics of the process. By defining the dimensionless groups, the way in which they were defined for one recycle case earlier, one gets

$$\frac{dx}{dt} = \lambda_1 \gamma x|_{t-\tau_1} + \lambda_2 \gamma x|_{t-\tau_2} - \gamma x + (1-x) y^2 \qquad (20)$$

$$\frac{dy}{dt} = (1-\lambda)\beta_1 \gamma - \gamma y + \lambda_1 \gamma y_{|_{t-\tau_1}} + \lambda_2 \gamma y_{|_{t-\tau_2}} + (1-x) y^2 - \alpha_1 y \qquad (21)$$

Here the $\tau_1 = 1080$ is chosen which exhibits bursting solution (corresponding to $\lambda_1 = 0.5$) and a second recycle stream with $\tau_2 = 2000$ and $\lambda_2 = 0.5$. In the fig5a and 5b the effects of second recycle are depicted, fig. shows that with the induction of second recycle term nature of solutions changes completely.

2.11 References

1. Goodwin B. C. Adv. Enz. Reg. 3 (1965) 425.

2. Goldbeter A., Nicolis G. Prog. Theor. Biol.4 (1976) 66.

3. Lewis E. R. Ecology 58 (1977) 738.

4. van Kampen Adv. Chem. Phys.24 (1976) 245.

5. White, B. S., S. I. A. M. J. Appl. Math. 32 (1977) 666

6. El'sgol'ts, L.E. and S. B. Norkin (1973) *An introduction to the theory and Application of differential Equations with deviating arguments.* Academic Press, New York.

7. Lewis E. R. Ecology 53 (1972) 797.

8. Glass L. and Mackey M. C., Science 197 (1977) 287.

9. (a) K. Ikeda and M. Mizuno, Physical Review Letters 53 (1988) 1340.
(b)C. Marriott, R. Vallee, and C. Delisle Physical Review A 1989, Volume 40, Number 6, 3420.

10. R. May, Nature 261 (1976) 459.

11. Noyes, R.M.; Field, R.J.; Koros, E. J. Am. Chem. Soc. 94 (1972) 1394.

12. Epstein, I.R.; Orban, M.; *Oscillations and Travelling Waves in Chemical Systems*; Field, R.J.; Burger, M., Eds.; Wiley: New York, 1984.

13. (a) Lintz, H.G.; Weber, W. Chem. Eng. Sci. 35 (1980) 203. (b) Papsin, G.A.; Hanna, A.; Showalter, K. J. Phy. Chem. 85 (1981) 2575.

14. (a) Aarons, L.J.; Gray, B.F. Chem. Soc. Rev. 5 (1976) 359. (b) Semenov, N.N. *Chain reactions*: Clarendon Press: Oxford 1935.

15. (a) Graziani, K.R.; Hudson, J.L.; Schmitz, R.A. Chem. Eng. J. 12 (1976) 9 (b) Sorensen, P.G. Proc. Faraday Soc. Symp. 9 (1974) 88.

16. Bar-Eli, K.; Noyes, R.M. J. Chem. Phys. 88 (1988) 3646.

17. Boissonade, J. J. Chim. Phys. 73 (1976) 541.

18. (a) Janz, R.D.; Vanecek, D.J.; Field, R.J. J. Chem. Phys. 73 (1980) 3132. (b) Rinzel, J.; Troy, W.C. J. Chem. Phys. 76 (1982) 1775.

19. (a) Winfree, A.T.; *The Geometry Of Biological Time*; *Biomathematics* Springer-Verlag: New York, 1980 8. (b) Pavlidis, T. *Biological Oscillators; Their Mathematical Analysis* : Academic Press: New York, London, 1973

20. Honerkamp, J.; Mutschler, G.; Seitz, R. Bull. Math. Biol. 47 (1985) 1.

21. MacDonald, N. *Time Lags in Biological Models*: Lecture Notes in Biomathematics: Springer: NewYork, 1978, 27.

22. Goel, N.S.; Maitra S.C.; Montroll, E.W. Rev. Mod. Phys. 43 (1971) 231.

23. Esteve, D.; Devoret, M.H.; Martinis, J.M., J. Phys. Rev. B. 35 (1986) 158.

24. Inamdar, S.R.; Ravi Kumar, V.;, Kulkarni, B.D.; Chem. Eng. Sci.,46 (1991) 901.

25. (a) Griffith, J.S. J. Theor. Biol. 20 (1968) 202. (b) Landahl, H.D. Bull. Math. Biophys. 31 (1969) 775.

26. Schell, M.; Ross, J.; J. Chem. Phy. 85 (1986) 6489.

27. Bellman, R.; Cooke, K.; *Differential Difference Equations*: Academic: New York, **1963**.

28. Gray, P.; Scott, S.K. Chem. Eng. Sci., 38 (1983) 29.

29. (a) Hodgkin, A.K.; Huxley, A.F. J. Physiol. (London) 117 (1952) 500. (b) FitzHugh, R. Biophys. J. 1 (1961) 445.

30. (a) Gray, P.; Scott, S.K. J. Phys. Chem. 89 (1985) 22.
(b) Balakotaiah, V. Proc. R. Soc. Lond. A411 (1987) 193.

31. Kevrekidis, I.G.; Schmidt, L.D.; Aris, R. Chem. Eng. Sci., 41 (1986) 41, 1253.

32. Bar-Eli, K. *J. Phys. Chem.* **1984**, 88, 3612.

CHAPTER III

SELECTIVITY BEHAVIOUR OF A MULTI-STEP REACTION ON A CATALYST MODELLED AS A **DLA** FRACTAL SURFACE

In the present chapter the idea of Fractals is introduced. In the case study, dynamics of a three step catalytic reaction on a DLA fractal has been simulated on a computer using random walks. The effects of varying probabilities of reaction steps and rate constants on the selectivity (ratio of the products formed) has been also analysed. Regions are isolated where maxima and minima of selectivity occur.

3.1 Introduction

A variety of systems in nature exhibit self similarities over extended ranges of spatial and temporal scales. The concept of fractal is used to describe these self-similar spatial organisations while $\frac{1}{f}$ like power spectra have been used to characterize self-similar temporal sequences[1]. In the real world many systems are far from perfectly ordered symmetry and far from equilibrium. Some examples are formation of dust, soot, colloids, bacterial cell colonies etc.

An object normally considered as one dimensional, a line segment, for example, possesses a scaling property (refer to figure 1). It can be divided into N identical parts each of which is scaled down by the ratio of r = $\frac{1}{N}$ from the whole. Similarly, a two dimensional square and a three dimensional cube can also be divided into N self-similar parts which are scaled down by a factor $\frac{1}{\sqrt{N}}$ and $\frac{1}{3\sqrt{N}}$ respectively. Now with self-similarity the generalization to fractal dimension is a straight forward. A D- dimensional self similar object can be divided into N smaller copies of itself each of which is scaled down by a factor r where r = $\frac{1}{D\sqrt{N}}$ or

$$N = \frac{1}{r^D}$$

Conversely, given a self-similar object of N parts scaled by a ratio r from the whole, its fractal or similarity dimension is given by

$$D = \frac{\log(N)}{\log\left(\frac{1}{r}\right)}$$

Take a simple straight line divide it into three parts (refer fig.2). Replace the middle segment by two equal segments forming part of an equilateral triangle. At the next stage in construction each of these four segments is replaced by 4 new segments with length $\frac{1}{3}$ of their parent according to the original pattern. This procedure is repeated over and over to yield beautiful Koch curve[1] as depicted in figure 2. Unlike Euclidian shapes this curve has details

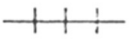

1-D N parts, scaled by ratio $r = 1 / N$

$N r^1 = 1$

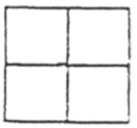

2-D N parts, scaled by ratio $r = 1 / N^{\frac{1}{2}}$

$N r^2 = 1$

3-D N parts, scaled by ratio $r = 1 / N^{\frac{1}{3}}$

$N r^3 = 1$

GENERALIZE

for an object of N parts, each scaled down by a ratio r from the whole

$$N r^d = 1$$

defines the fractal (similarity) dimension D

$$D = \frac{\log N}{\log 1 / r}$$

Figure 1 Interpretation of standard integer dimension figures in terms of exact self-similarity and extension to non integer dimensioned fractals.

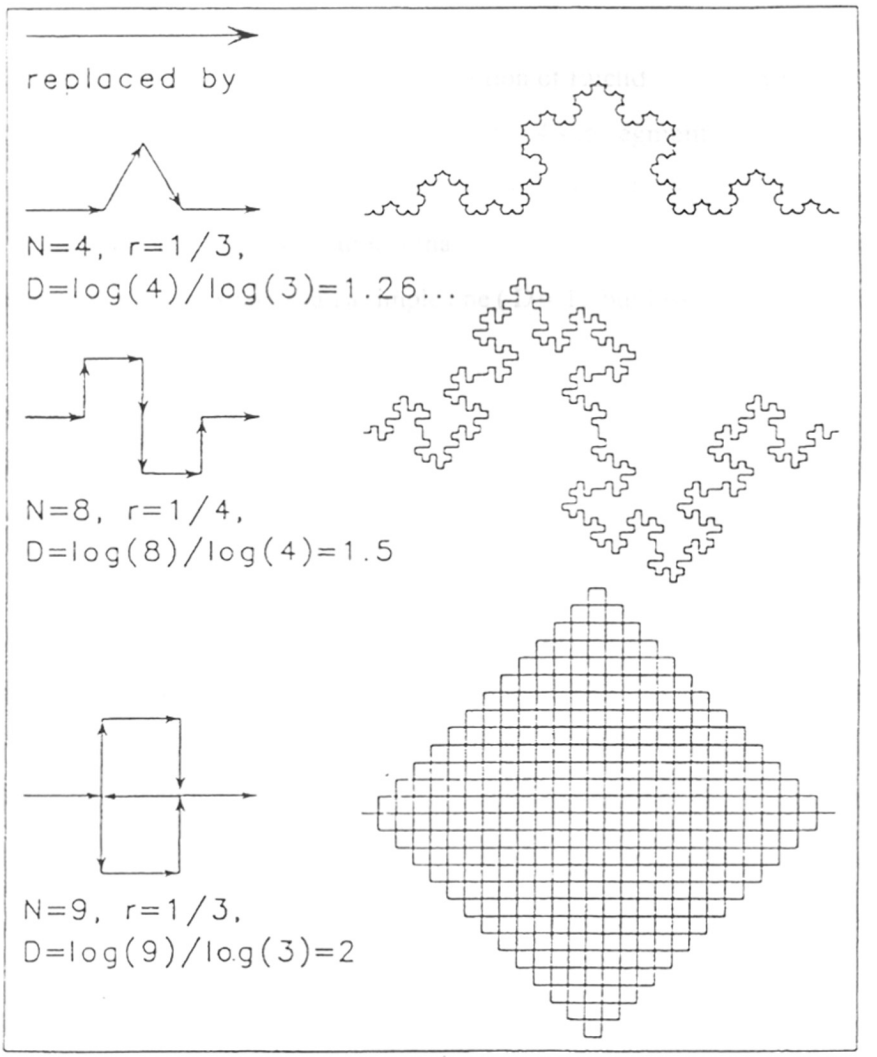

Figure 2 Recursive replacement for generating the von Koch snowflake curve and variation with different fractal dimension.

on all length scales. Each small portion when magnified, can reproduce exactly the larger portion. The curve possesses an exact self-similarity. Also at each stage of construction the length of the curve increases by a factor of $\frac{4}{3}$.

The fractal dimension, unlike the more familiar notion of Euclidian dimension, need not be an integer. Any segment of Koch curve is composed of 4 sub-segments each of which is scaled down by a factor of $\frac{1}{3}$ from its parents. Its fractal dimension is $D = \frac{\log(4)}{\log(3)}$ or about 1.26. This non-integer dimension, greater than 1 but less than 2, reflects the unusual properties of the curve. It somehow fills more of space than a simple line (D= 1), but less than a Euclidian area of a plane (D = 2).

The exactly self-similar von Koch curve has been considered as a crude model for a coastline, although it differs from the coastline in one significant aspect. Upon magnification segments of the coastline look alike, but never exactly the same. They are self similar only in a statistical sense. The concept of fractal dimension, however, can also be applied to such statistically self-similar objects. In a measurement of the length of a coastline, the more carefully one follows the smaller wiggles, the longer it becomes. A walk along a beach is longer than the drive along the corresponding highway. When using a ruler of size r to measure a coastline's length, the total length equals the ruler size r times the number of steps of size r, N(r)

$$Length = r.N(r)$$

$$Length \alpha r.\frac{1}{r^{D}} = \frac{1}{r^{D-1}}$$

Thus, for D > 1, as the size of the ruler used to measure a coast decreases, its length increases. Real coastlines can in fact be characterizes by fractal dimension D of about 1.15 to 1.25[2].

The property that the objects can look statistically self-similar while at the same time different in detail at different length, is the central feature of fractals in nature. The concept of fractals has found a widespread application in several branches of science and engineering. A few of these applications are summarized in the next section.

3.2 Applications

3.2.1 Molecular recognition studies

One important aspect of structure is understanding the physico-chemical basis for the specificity of molecular interactions and mechanism of recognition. Undoubtedly, an essential step in this process is the formation of complementary contacts between approaching molecular surfaces. Surface representations of proteins have provided a powerful tool for characterization of stretching, folding and various interactions of proteins. A feature of surfaces that has recently been described is texture i.e. roughness of protein surface[3]. Categorization of surface morphology or texture has been made feasible by fractal dimension. Surface irregularity of the protein are approximately of same scale as water molecule or small ligands. Literature cites the cases wherein the fractal dimension of the active site is different the rest of the protein

3.2.2 Shape of Bacterial Colonies

A large number of bacterial colonies have fractal shapes[4]. In these studies the fractal concept serves a useful measure to quantify the extent of effect of environment on bacteria, production of extracellular compounds. The results from these studies are going to be useful in biochemical engineering, especially in large scale reactor studies and membrane separation.

3.2.3 Fractal kinetics

Classical reaction kinetics has been found to be unsatisfactory when reactants are spatially constraints on the microscopic level either by walls, phase boundaries or force fields. Recently discovered theories of heterogeneous reaction kinetics have dramatic consequences,

such as fractal order of reaction, self ordering and self unmixing of reactants and rate coefficients with temporal memories (whereas in classical kinetics, we do not expect rate constant k, to have any time dependence[5].

3.2.4 Dynamical Models

In dynamical systems, the instantaneous state of the system can be represented by a point in the phase space. An attractor is a sub-space of some ordinary N-dimensional space to which the solution of an N-dimensional system asymptotes for large times. The cases when the system is exhibiting chaotic behaviour, the attractor of the system possesses a non-integral fractal dimension. Although, the chaotic temporal behaviour essentially represents the dynamics of system, the strange attractor which has non-integral dimensionality i.e. fractal in character is a static object. This property of the fractals will be treated in subsequent chapters.

3.3 Fractal growth models

Practically all forms in nature are product of some kind of growth. Growth means history. The end product depends on certain configuration of the past. This means that the configuration at the given time are not independent from each other but are correlated, through history, in a complicated way. A process like this is called non-Markovian. So it is not in general possible to simply write down a partition function or generating function. Growth models, can be characterized based on mechanisms based on energetic consideration i.e. which include temperature(ex. Nucleation or crystallization). Another classification of growth models is based on purely random kinetic mechanism (also called geometric growth models because kinetic mechanism depends only on the geometric features of the clusters like surface, position of growth sites, steric hindrance effect etc..

3.3.1 Geometric Growth Models

Aggregation: Here one considers many moving particles or clusters and when two of them touch each other, they might stick together, growing thus to a larger unit

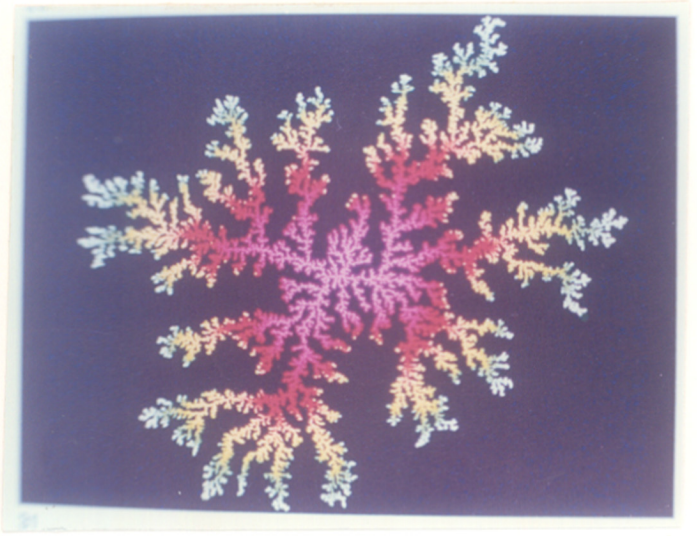

Figure 3 Diffusion limited aggregation (DLA) of 5000 particles on a square lattice.

Gelation: In gelation model one has many growing clusters which crosslink forming a network. Some other models which do not belong to either of these classes are Epidemics, Electrical Breakdown etc.

3.4 Case Study

Present work is confined to models where only one cluster grows. They exhibit an exact scaling behaviour which technically occurs only after an infinite number of growth steps. The scaling is characterized by critical exponents. Examples of these models include Eden model and DLA. The aggregates which are formed due to the irreversible flocculation of colloidal particles frequently exhibit the self similarity of fractal structures[6]. A simple stochastic model known as diffusion limited aggregate (**DLA**) for the formation of such aggregates of particles in two-dimensional space was proposed by Witten and Sander[7]. In DLA processes, a cluster is grown from a seed particle as randomly walking (i.e. diffusing) particles launched from distant positions arrive at and stick to the surface of aggregate. The pattern of clusters produced by DLA processes have random and ramified structures. The total number of particles N deposited in the aggregate grown on a single seed can be scaled down with linear size R of the aggregate as $N \sim R^{D}$. Computer simulation[8a] extended to higher Euclidian dimensions (d= 2 to 6) have shown that the fractal dimension of the aggregates is given approximately by $D \sim \frac{5d}{6}$. Several experiments relevant to DLA have so far been performed , such as dielectric breakdown[8b] , electrodeposition[8c] and viscous fingering[8d]. This model is found to be applicable to a metal-particle aggregation process. The preparation methods for catalyst or catalyst support can be modelled by random process simulations that generate such self-similar or fractal structures. The reaction-diffusion or adsorption diffusion on the catalysts possessing fractal shape may be accounted for via several approaches, one of them being direct stochastic simulation which takes into account the random motion and reaction probability[9a,9b].

The motivation for this work is to analyse the dynamics of a three- step surface reaction taking place on catalysts having a DLA type geometry with a view to establish the relationship between selectivity and reaction probabilities.

3.5 Model

The model reaction considered for analysis is given by

$$A + S - - - \rightarrow A_a \quad (1)$$

$$A_a - - - \rightarrow B \quad (2)$$

$$A + A_a - - - \rightarrow C \quad (3)$$

Here, A represents the reacting particle, S the fractal surface site and B and C the products. The selectivity is defined as the ratio of the number of C molecules produced to that of B molecules produced. The case where steps (1) and (3) occur with probability one has been analyzed by Meakin[9a] on DLA and percolating clusters. In reality it is more likely that all collisions may not be reactive. In the present work we, therefore, assign certain probabilities for step (1) and (3) and simulate the performance.

3.6 Numerical procedure

A random fractal structure (DLA fractal) has been generated on a two dimensional square lattice using the methodology given by Witten Jr. and Sander[7a]. The precaution that the perimeter sites near the center get " screened" has been taken so that the exposed ends of the cluster grow more rapidly. Fig 3 shows a typical two-dimensional DLA fractal produced by 5000 particles over a square 200 x 200 lattice adopting this procedure. The fractal dimension for such clusters has been computed to be equal to 1.70 ± 0.03.

In order to simulate the reaction, the following methodology has been employed: Let us define the probabilities of the reaction (1) and (3) to be equal to P_1 and P_3 respectively. The molecule (particle) A starts its random walk on the random fractal from outside the rectangular area defined by fractal boundaries. Periodic boundary conditions ensured that the simulated system is effectively part of an infinite system. If this random-walking particle comes onto site occupied by the fractal, it gets adsorbed with probability P_1. This can be

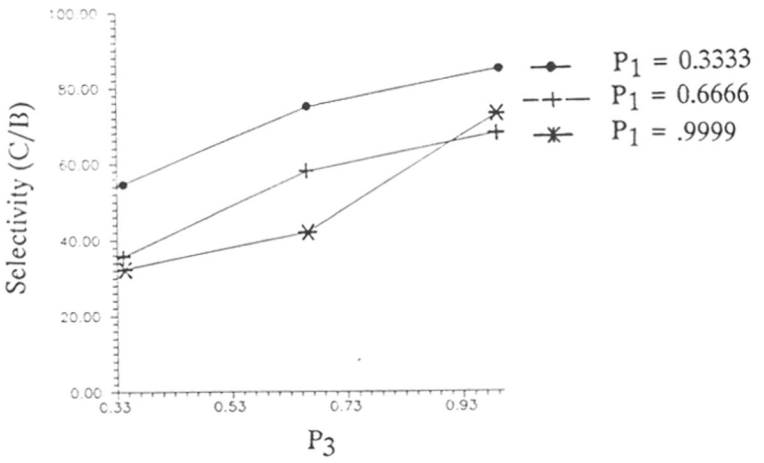

Figure 4 Selectivity as a function of P_1 and P_3.

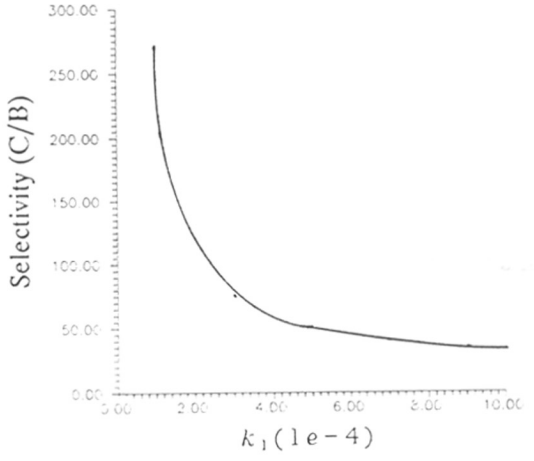

Figure 5 Selectivity as a function of rate constant k_1.

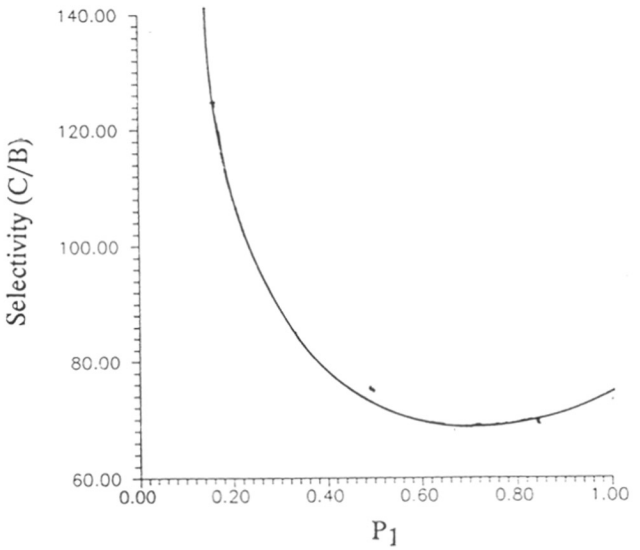

Figure 6 Selectivity as a function of P_1 for $P_3 = 1$.

achieved by generating a random number when the particle visits the fractal site and checking whether it is less than P_1, then the particle stays adsorbed or continues its random walk (with probability $1 - P_1$).

In the event when reaction (1) takes place, reaction (2) follows and the number of B molecules produced (N_B is increased by the product of $k_1 N_{A_{ad}}$ The term $N_{A_{ad}}$ refers to the total number of adsorbed A molecules on the fractal surface and k_1 denotes the rate constant for the reaction step (2). When N_B increases by the integer 1, a randomly chosen adsorbed A site is converted into B molecule and the time also increments by 1. In this way, we can account for the rate constant for reaction (2).

A randomly moving A particle can also visit the fractal site on which an A molecule has already been adsorbed, in which case reaction (3) takes place. A random number is generated in case of such an event and checked whether it is less than the probability P_3 for the reaction (3). If this check is positive, then the number of C molecules produced N_c and the time are incremented by 1.

We have assumed for these simulations that the B and C molecules, once generated, get desorbed immediately and therefore a randomly chosen adsorbed A fractal site is vacated. When a moving A particle travels sufficiently far away from the cluster, there is a very low probability of any of the reactions taking place, and hence a new A particle is launched in the vicinity of the cluster. If this random walk results in any of the reactions, the same procedure as outlined above is followed except that the time is not incremented. In the simulations that have been carried out, a large number of A particles were launched until the system attained steady state and the selectivity, as defined by the ratio of $\frac{N_C}{N_B}$, estimated. Approximately 500000 trajectories of A molecules are required before the system reaches the steady state.

3.7 Results and Discussion

In the present work we have analyzed the effects of varying P_1 and P_3 on the selectivity of the reaction products. The case where the best selectivity is obtained has then been considered in order to observe the effects of variations in the rate constant k_1 for the step (2). All the simulation have been carried out on DLA clusters having 2400 sites.

The probability P_1 was held constant at 0.3333 and P_3 was varied between 0.3333 to 1 at intervals of 0.3333. The rate constant k_1 for the reaction A_s--> B was taken to be equal to 0.0003. For two other values of P_1 (0.666666 and 1) the same procedure was repeated. Every case was simulated on different DLA clusters (generated using different sets of pseudo-random numbers keeping the same total of fractal sites) and selectivities were averaged. Fig.4 give the plot of the results of these studies. It can be seen that as the probability for the reaction (3) increases for a given value of P_1, there is an enhancement in the selectivity. The highest selectivity is obtained for $P_1 = 0.333$ and $P_3 = 1$. Figure 5 shows a selectivity versus rate-constant plot for $P_1 = 0.3333$ and $P_3 = 1$. It can be easily seen that as the rate constant increases , the selectivity drops. The decrease is, however, sharp in the range of $k_1 =$ 0.0001 to 0.0003. It is obvious that higher values of k_1 will result in the enhanced production of B molecules and will lower the selectivity.

It is noticed from Fig.4 that for $P_1 = 0.3333$ and $P_3 = 1$, there is a cross over and the corresponding selectivity is greater than for $P_1 = 0.6666$ and $P_3 = 1$.

In order to investigate this further, studies for a fixed value of $P_3 = 1$, with varying P_1 were conducted. Fig. 6 shows the results of these simulations. The selectivity has been found to go through a minimum as P_1 is increased beyond 0.5. The explanation for the occurrence of such a situation can be given in physical terms. If P_1 is lower than, say, 0.1666, then out of every 10000 particles of A, 1666 have a chance to get adsorbed. The remaining particles are therefore available as free A particles. Note that the rate of formation of C particles depends both on adsorbed A and the free particles of A on fractal surface. With an increase in

probability for the first reaction step, although, A_α increases, the free A particle concentration declines. There is, therefore, an optimal value for the probability of reaction step (1) which maximizes the C formation. Alternatively, for certain other combinations of number of free A particles and number of A adsorbed, we get a minimum in the selectivity. Notice also that the formation of B depends solely on the amount of A_α.

In conclusion, the work reports the results of simulation studies for a three-step reaction on a catalyst surface modelled as a DLA fractal object. The inclusion of probabilities with which different reaction steps can occur leads to a situation of a maximum and minimum in the selectivity

3.8 References

1. M.F. Barnsley, R.L. Devaney, B.B. Mandelbrot, H.O. Peitgen, D. Saupe, R.F. Voss,(1988) *'The Science Of Fractal Images'*, Springer-Verlag.
2. B.B. Mandelbrot, (1982), *'The Fractal Geometry Of Nature'*, W.H. Freeman and Co., New York.
3. M.Lewis and D.C. Rees Science 230(1985) 1163-1165.
4. Tohey Matsuyama, Masakaju Sogawa and Yoji Nakagawa FEMS Microbiology letters 61 (1989) 243.
5. Roul Koupelman, J. Stat. Phy. 42(1986) 185., P. Klymko and R. Koupelman, J. Phy. Chem. 86 (1982) 3686; 87 (1983) 4565.
6. D.A. Weitz, M.Y. Lin, J.S. Huang,T.A. Witten, S.K. Sinha, J.S. Gethner and R.C. Ball in *Scaling Phenomena in Disordered Systems*, eds., R. Pynn and A. Skjeltorp, NATO Advanced Institute Series B, Vol. 133 (Plenum Press, New York, 1986
7. (a)T.A. Witten Jr. and L.M. Sander, Phys. Chem. Rev. 47,(1981) 1400, (b)T.A. Witten Jr. and L.M. Sander, Phys. Rev. B 27(1983) 5686.
8. (a)L. Niemeyer, L. Pietronero and H.J. Wiesman : Phys. Rev. Lett. 52,(1984) 1033.

(b)M. Matsushita, M. Sano, Y. Hayakawa, H. Hanjo and Y. Sawada Phys. Rev. Lett. 53 (1984) 286.

(c) R.M. Brady and R.C. Ball, Nature 309 (1984) 225.

(d) J. Nittsmann, G. Daccordand H.E. Stanley: Nature 314 (1985) 141

9. (a)P. Meakin, Chem. Phys. Letters 123 (1986) 428.

(b) M. Sheintuch and M. Brandon, Chem. Eng. Sci. 44 (1989) 69.

CHAPTER IV

CHAOTIC DYNAMICS

Present chapter introduces the idea of chaotic dynamics, its origin and significance. Methods to quantify chaotic dynamics are also studied. The glycolytic model as given by Sel'kov is taken as representative case. Parameters corresponding to various dynamic modes are isolated, which will form the groundwork for the next chapter.

4.1 INTRODUCTION

According to traditional views, the frequencies present in the time evolution of a system correspond to excitation of various modes or degrees of freedom of the system. Following these views, hydrodynamical turbulence was thought due to excitation of a large number of modes of a fluid which, being a continuous system has indeed an infinite number of degrees of freedoms. This is the theory of Landau and Hopf. It has, however, been realized now that dynamical systems with low dimensional phase space (dimensionality $>/=3$) may already have a continuous superposition of different frequencies. Systems with a small number of degrees of freedom may thus exhibit a turbulent time behaviour. Homogeneous chemical systems have a priori only a finite number of degrees of freedom at their disposal. The classical view going back to Boltzman, Gibbs, Einstein and Landau that the irregular behavior in nature results of necessity from interaction of a large number of degrees of freedom has been shaken recently. Very simple deterministic nonlinear models can have extremely complex and irregular behaviour, and irregular behavior is rule, regular behaviour is exception. According to new description, as few as three degrees of freedom suffice by interacting nonlinearly, to create 'deterministic chaos' also referred in literature as deterministic stochasticity or turbulence[1-6]. In this phenomena self-similarity is believed to occur in both space and time[7,8].

One of the main outcomes of the research in macroscopic systems is that we live in a pluralistic universe, we deal with both dissipative and conservative systems which have widely different properties. Briefly, dissipative systems are characterized by asymptotic stability. They forget temporary perturbations. The simplest example is a pendulum with friction. If perturbed it goes back to equilibrium position. The equilibrium position is a point attractor, however, we know now that attractors may be more complicated than isolated points. They may be lines in phase space, such as periodic chemical reaction or even more complicated mathematical objects like fractals, also called strange attractors[7]. The second common element in the dissipative systems is dissymmetry with respect to the time. All dissipative systems have the preferential direction of time, they progress towards the attractor as time goes from t to infinity[9]. In classical mechanics conservative system would be described by time independent Hamiltonian. From abstract point of view, such systems are characterized by a phase space and by a measure which is preserved in time. A striking difference is that the conservative dynamical systems are never stable in the same sense as dissipative systems. They do not have a property of asymptotic stability. When we give a larger amplitude perturbation to a frictionless pendulum, it takes a new frequency and conserves it as long as friction can be neglected. On the contrary, if we run, our heart beat increases but returns to normal after we take rest. Thus there is no fluctuation-regression mechanism in conservative systems, and they

are basically unstable. Around the turn of the century Poincare[10] and others recognized that much could be learned about dynamical behavior from an analysis of system trajectories in a multidimensional phase space in which a single point characterizes the entire system at an instant of time. The set of phase space trajectories for all possible initial conditions (for a given set of control parameter values) forms the phase portrait of the system. This invariant set is also called an attractor, the trajectories rapidly return to this limit set after finite perturbations. The basin of attraction is the set of all initial points for which the trajectories asymptotically approach the attractor. Thus we distinguish the global and local attractor. In the systems fully described by a scalar or a two-component vector order parameter, they can only give rise to attractors in the form of fixed points or limit cycles. This is mainly due to the topological constraints imposed on the trajectories in a one or two dimensional phase space, being understood that self-intersections are not allowed by the uniqueness theorem.

Consider a non linear dynamical system evolving according to certain laws given by

$$\frac{dX}{dt} = F(X, \lambda) \tag{1}$$

in this $\mathbf{X} = \text{col}\,(X_1, X_2, X_3, \ldots X_n)$, $\mathbf{F} = \text{col}\,(F_1, F_2 \ldots F_n)$ and λ denotes a set of parameters. Suppose that the system has reached a particular state X_s. In a conservative system it could represent the state of mechanical equilibrium. In a dissipative system it could represent the state of thermodynamic equilibrium or a nonequilibrium state, for instance by imposing a fixed external constraint. Numerous experimental results have shown that in the latter case the system can admit, for an appropriate range of constraints values, a time-independent regime referred to as stationary non equilibrium state.

In actual fact, a real world system never stays in a single state as time varies. To begin with, most systems are in contact with a complex or even unpredictable environment. This environment continuously communicates to them slight (or more rarely, strong) quantities of matter, momentum or energy, as a result of which it becomes practically impossible to control any of the state variables with an unlimited precision. We can say this fact that state of our system is not X_s but, rather, a nearby X related to X_s through

$$X(t) = X_s + x(t)$$

The quantity x will be referred to as perturbation. Typically, a fluctuation originates in the form of a localized small scale event. The response of the system to the fluctuation can be studied in terms of its effect on either a particular reference state or on the sequence of

states defining a trajectory. Thus enters the idea of asymptotically stable and asymptotic orbital stable. In both of these cases the perturbation x(t) decays to zero in time. Similarly we can have unstable fixed points and unstable orbits. Dissipative dynamical systems are capable of eliminating the effects of perturbation that may act on them and reestablish in this way the reference state. This ensures the predictability and reproducibility of this regime, which is referred as **attractor.** One can easily realize that asymptotic stability is one of the most striking manifestation of the constructive role of irreversibility in nature[2,9].

4.2 Strange Attractors

When a dynamical system evolves in a phase space of three or more dimensions, the topological constraints arising from the non-intersection of the trajectories are greatly relaxed and, as a result, a new kind of behavior known as chaotic dynamics can arise. Turbulence, one of the universal properties of large scale flows, is the most familiar example of a well defined dynamical system whose state variables show an apparently erratic behavior in phase space. For a dissipative systems the volume occupied by the attractor is very small compared to the volume of the phase space, here the phase space volume gets contracted by the time evolution. Even if a system contracts volumes, this does not mean that it contracts lengths in all directions. Intuitively, some directions may be stretched, provided some other are so much contracted that the final volume is smaller than the initial volume. This seemingly trivial remark has profound consequences. It implies that, even in a dissipative system, the final motion may be unstable within the attractor. This instability usually manifests itself by an exponential separation of the orbits (as time goes on) of points which initially are very close to each other (on the attractor). The exponential separation takes place in the direction of stretching, and an attractor having this stretching will be called strange attractor. Of course, since the attractor is in general bounded, exponential separation can only hold as long as distances are small. For an explanation of irregular behaviour, so called hyperbolicity condition play a crucial role. They say, in intuitive terms that near any fixed trajectory the neighbouring trajectories behave like a saddle point. If this is the case then at every point in the state space, the trajectories necessarily get mixed up and show stochastic behaviour. Chaos contains an infinity number of unstable periodic orbits which characterize it. The natural measure of a region of an attractor is the probability that a long chaotic orbit visits that region. Scaling properties of the probability are related to the local expansion rates of nearby orbits in the stretching and contracting directions.

Sensitivity to initial conditions is one of the most important characteristic of a chaotic dynamics. Two closeby trajectories diverge exponentially with time, the rate of divergence being characterized by the Liapunov exponents[11a,11b]. Thus a small initial uncertainty in the initial conditions grows rapidly and after some time it becomes almost impossible to predict

the phase space trajectory. We may say that system progressively loses the memory to initial conditions. The time required to lose the memory of the initial conditions depends on the rate of divergence of the trajectories and the amount of uncertainty in the initial conditions.

Strange attractors have various kinds of scaling properties in temporal and spatial scales. The stretching processes have turned out to be characterized by a temporal scaling exponent which represents the spectrum of fluctuations of local expansion rate in the stretching direction. On the other hand, the folding processes produce numerous singularities of the probability measure on strange attractor, and have been found to be characterized by a spatial scaling exponent which represents the fractal dimension of a set of singularities with a scaling exponent. This spectrum is related to the generalized dimension of the attractor and is useful for analysis of multifractals appearing in chaos[12,13]. A very peculiar feature of a strange attractor which distinguishes deterministic chaos from a random process is its fractal (Hausdorff- Besicovitch) dimension. The dimension of an attractor is clearly the first level of knowledge necessary to characterize its properties. We may think of dimension as assigning in some way the amount of information necessary to specify the position of a point on the attractor to within a given accuracy. The dimension is also the lower bound on the number of essential variables needed to model the dynamics. For simple attractors, defining and determining the dimension is easy. For example, using any reasonable definition of dimension, a stationary time independent equilibrium (fixed point) has dimension zero, a stable periodic oscillation (limit cycle) has dimension one, and a doubly periodic attractor (2- torus) has dimension two. It is because their structure is very regular that the dimension of these simple attractors take on integer value. Chaotic (strange) attractors, however, often have a structure that is not simple, they are often not manifolds, and frequently have a highly fractured structure. For chaotic attractors, intuition based on properties of regular and smooth surfaces does not apply. The most useful notions of dimension takes on values that are typically not integers. To fully understand the properties of chaotic attractor, one must take into account not only the attractor itself, but also the distribution or density of points on the attractor. This is more precisely discussed in terms of what we call the natural measure associated with the given attractor. The natural measure provides a notion of the relative frequency with which an orbit visits different regions of the attractor[15a]. Most of the dimensions of natural measure are very difficult to compute by box counting algorithms, as this is a method very consuming of memory and it is impractical for a phase space dimension greater than two. Thanks to the Kaplan-Yorke conjecture[14] the dimension of the chaotic attractor can be determined in from the dynamics in terms of Liapunov exponents.

4.3 Chaos in terms of information flow

In classical mechanics the energy in a system is divided into macroscales and microscales. The energy of microscales are uncertain by roughly kT, but this is small compared to the amount of energy per degree of freedom they usually contain, and is successfully neglected, thus it is possible to predict essentially completely the future behavior of the macroscopic degrees of freedom using only the complete initial knowledge of these same scales. There are, however many nonconservative systems for which this implicit separation breaks down[15b] there may be an active flow of information between macro and microscales. Information occurs in the context of messages and measurements. If we assign probabilities p_i to each of the possible outcomes, then we can define the information associated with the outcome as

$$H = -\sum_{x=0} P_i \log_2 P_i$$

This definition has the property that if we have a completely determined outcome, with a probability unity, the information content is zero. We learn nothing new from the message, thus it contains no information. It is sometimes said that information is the measure of surprise of an occurrence, the less a priori knowledge we have, the more information it contains. In this definition the units of information are 'bits', the information contained in the outcome of an even binary experiment, such as an unbiased coin flip. It is clear that as we increase the accuracy of measurement, information obtainable also increases. Classically one can raise the information to an arbitrarily high value by taking higher precision of the measurement. Practically, however we soon reach a limit, in a given measurement situation the Uncertainty Principle tells us the theoretical resolution limit which can be approached but never surpassed. The physical nature of the reality limits the information we can learn about a given system to a particular number. Extending this idea to phase space, we can divide the phase space into blocks of minimum size. In statistical mechanics these blocks are referred as states. One can see that some accessible information gets destroyed by the contracting flow in phase space, and by get created by the expanding flow.

4.4 Analogy with Phase Transitions

Phase transitions occur at certain value of control parameter, T or P, when latter is subjected to a slow and progressive variation. Many thermodynamical quantities show singular behaviour when absolute $T - T_c$ tends to zero. Here T_c is the critical point. Chaotic transitions also takes place at μ_c critical value of control parameter, such as Reynolds number and shows singularity at absolute value $\mu - \mu_c$ tending to zero. The formation of the new phase may be described by appearance of non zero 'order parameter', say macroscopic magnetization

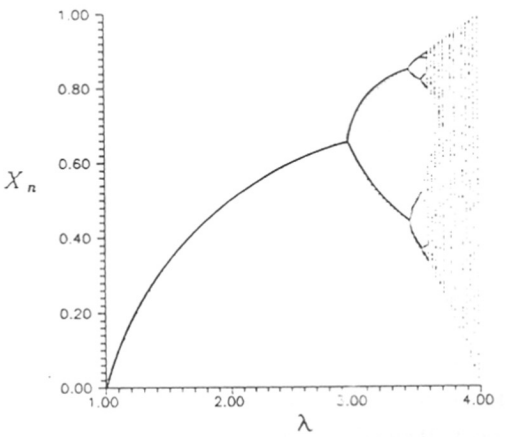

Figure 1 Bifurcation Sequence for X_n versus parameter λ for the Logistic Map.

in ferromagnetic phase transitions. In fact Liapunov Exponents correspond to the reciprocal of the correlation length ζ in phase transitions. An important notion in phase transition theory is the correlation length ζ which diverges at the critical point as

$$\zeta \propto (T - T_c)^{-\nu}$$

where ν is a positive universal constant. We also know that when Liapunov exponent is negative, system approaches an asymptotic stable state independent of initial conditions, and the influence of initial conditions quickly decays. When L.E. is positive, nearby orbits run away exponentially and any minor change in the initial conditions will be amplified with time. Therefore λ^{-1} can be taken as a measure of time correlation i.e. more the value of L.E. faster will be the correlation decay. A further impetus for the analogy between transition to chaos was given by Huberman and Rudnick[17], by the observation that as the control parameter 'r' in the those models increases past a critical value r_c into the chaotic regime the L.E. has an envelop curve of the form $(r - r_c)^{\tau}$, the universal constant τ = 0.4498069. This behaviour is reproduced in Chapter six of the thesis.

4.5 A Case Example

Chaotic phenomena are not just a motley collection from mathematical labyrinth but a wide class of natural events found in the physical world. Chaos can be thought as a new regime of nonlinear oscillations, as a compromise between competiting periodicities, as overlap of resonances, as accumulation of many periodicities, as a prelude to turbulence. The determinism inherent in chaos implies that many random phenomena are more predictable than had been thought. The appealing aspect of chaos is that it offers a way to understand complicated behavior as something that is purposeful and structured instead of extrinsic and accidental. Random-looking information gathered in the past and shelved because it was assumed to be too complicated can now be explained in terms of simple laws. While the irregularity of chaos fascinates scientists at the same time they look for regularities. A very interesting regularity was found by Feigenbaum[16]. Consider the difference equation

$$x_{k+1} = r\, x_k (1 - x_k) \qquad (2)$$

It was shown that the value of the parameter at which the period of the attractor doubles from r^n to r^{n+1} obey simple rule in the system governed by the equation

$$\frac{r_n - r_c}{r_{n+1} - r_c} \text{ - - - - - - } \rightarrow 4.6692$$

r_c is the limiting value where chaos sets in. The bifurcation diagram depicting period doubling cascade is shown in figure 1.

4.6 Characterization of strange attractor

For an N-dimensional system, the N-Liapunov exponents quantify the sensitivity of system dynamics to its initial conditions and also indicate the degree to which nearby phase space trajectories diverge. Chaotic behavior is exemplified by the presence of atleast one positive Liapunov exponent and a zero exponent. The existence of more than one positive Liapunov exponents shows a hyperchaotic system and arises due to orbits diverging in multiple directions in phase space. Limit cycle or more complex multi-peak periodic situations have an associated zero valued exponent with all others negative while stable dynamics have all negative exponents. The evaluation of the Liapunov exponents from a known set of differential equations can be carried out by observing the evolution of small perturbations to the system orbit during its time evolution[11a,11b]. Thus if $J(x[t])$ is the $N \times N$ Jacobian matrix evaluated along a dynamic system orbit whose states are represented by the vector $x[t]$ then a perturbation, δx, to the orbit satisfies the relation

$$\delta x[t + \Delta t] = J(x[t])\,\delta x[t] \tag{3}$$

The divergence of nearby orbits can be studied by monitoring the growth rate of an infinitesimal N-dimensional hyper-sphere constructed about an initial state of the system trajectory by specifying a set of N orthonormal vectors ($\alpha_k[t]$, $k = 1, 2, \ldots N$) around this state. On solving the system equations with the N sets of linearized equations of motion [obtained in the form of eq. (3)] yield the growth rate of the these vectors in time. The hyper-sphere is seen to deform into an hyper-ellipse and the Osledec multiplicative ergodic theorem states that the characteristic radii of this hyper-ellipse converges in time. The Lyapunov exponents are related to the converged value of these radii. Let the norm $||\alpha_k(\infty)||$, $k = 1, 2, \ldots, N$ be the metric quantity measuring the magnitude of these radii vectors. The N Lyapunov exponents (λ_k, $k = 1, 2, \ldots N$), can be calculated as

$$\lambda_k = \lim_{t \to \infty} \frac{1}{t} \ln \frac{||\alpha_k[\infty]||}{||\alpha_k[0]||} \qquad (k = 1, 2, \ldots, N) \tag{4}$$

where if an orthonormal frame of reference is chosen, then, $||\alpha_k(0)|| = 1, k = 1, 2, \ldots, N$. To aid the numerical solution of the system eqs (1) employing a time interval Δt, the discretized version of eq. (4) may be written as

$$\lambda_k[t] = \frac{\sum_{1}^{r} \ln(||\alpha_k[\infty]|| / ||\alpha_k[0]||)}{r\Delta t} \qquad (k = 1, 2, \ldots, N) \qquad (5)$$

where as $t \to \infty$ eq. (6) converges to the Lyapunov exponents λ_k. Repeated applications of eq. (3) however, can lead an ill conditioned nature of the matrix $J(x[t])$. Moreover, due to the finite precision normally used in calculations we observe that each of the vectors $\alpha_k[t], k = 1, 2, \ldots N$ tends to align itself with the local direction of most rapid growth and effectively all the α_k converge to the largest Lyapunov exponent. Ortho-renormalizing the $\alpha_k[t], k = 1, 2, \ldots N$'s at frequent intervals can circumvent these problems and yield reasonable estimates of the exponents in decreasing order.

Kaplan and Yorke[14] have shown that there is a meaningful connection between the values of the Lyapunov exponents and fractal dimensions. According to them the Lyapunov dimension is related to the first i exponents which when summed up retains a positive value and the $(i+1)$ exponent by the following equation

$$D_L = i + \frac{\sum_{m=1}^{i} \lambda_m}{|\lambda_{i+1}|} \qquad (6)$$

Equation (6) suggests that exponents beyond $(i+1)$ are of lesser importance, since, the first $(i+1)$ exponents predominate both in specifying the phase space diverging properties and the self-similar properties associated with the fractal type structure of the attractor. Estimating values of D_L is consequently useful from a point of view of estimating the reduced dimensionality of the system after it has stabilized on the attractor manifold by a process of dissipation.

4.7 Model

One can not go very far in biology before stumbling on some periodic phenomena. These phenomena fulfil the thermodynamic requirement for dissipati ve structures i.e some inherent nonlinearity in the system kinetics and openness to mass and/or energy exchange with the surroundings. The nonlinear kinetics stems from nonlinear interactions of variables, feedback or feedforward loops, autocatalysis etc. Deterministic aperiodicity or chaos found in other disciplines of science is also not new to biosystems. More and more chaos reaches the scope of investigators working on mathematical or experimental models in biology[18a,18b]. To

reactions[18c], the Dictyostelium cAMP-system[18d], models of excitable membranes[18e,18f]. There are a few cases in which chaos has been observed experimentally. These examples come from studies in analysis of EEG data human brain[19a] while working on the K^+-selective conductance system of molluscan neuron[19b], population biology[20a,20b]. There are also cases of chaotic phenomena in many biological model systems which still await there experimental verification. Previously held notion that homeostatis is best for the individual is slowly being questioned. One justification comes from the control of chaos[21] where it is shown how presence of chaos can be of great advantage to the system. A chaotic attractor has within it an infinite number of unstable orbits. The human body can chose one of that unstable orbits which gives improved system performance. Now a time dependent small change in the parameter value can occur which will stabilize this orbit. Compare this with the situation wherein we have one stable limit cycle , a small time dependent parameter change can alter the orbit only slightly. Compared with the latter case a chaotic system is capable of showing the performance as required by cell's metabolism. In the glycolysis, phosphofructokinase reaction is commonly thought of as being a possible source of self oscillation[22]

$$\frac{dx}{dt} = 1. - Bx - xy^2 \tag{7}$$

$$\frac{dy}{dt} = A(xy^2 - y) \tag{8}$$

Here the nonlinearity is due to an autocatalytic reaction of the substrate x into the product y. Deterministic chaos was found in the extended model containing in addition to (7-8), a reversible deposition of x into an inactive form z. Denoting x, y, z by x_1, x_2, x_3

$$\frac{dx_1}{dt} = 1 - Bx_1 - x_1x_2^2 - Ex_1x_2 + x_3 \tag{9}$$

$$\frac{dx_2}{dt} = A(x_1x_2^2 - x_2 + G) \tag{10}$$

$$\frac{dx_3}{dt} = F(Ex_1x_2 - x_3) \tag{11}$$

A bifurcation diagram and some routes to chaos are discussed in[23]. In this reference the nonperiodic long-term behaviour was taken as indicator of chaos. In the present chapter characterization of this system will be done in terms of Liapunov exponents. Results will also

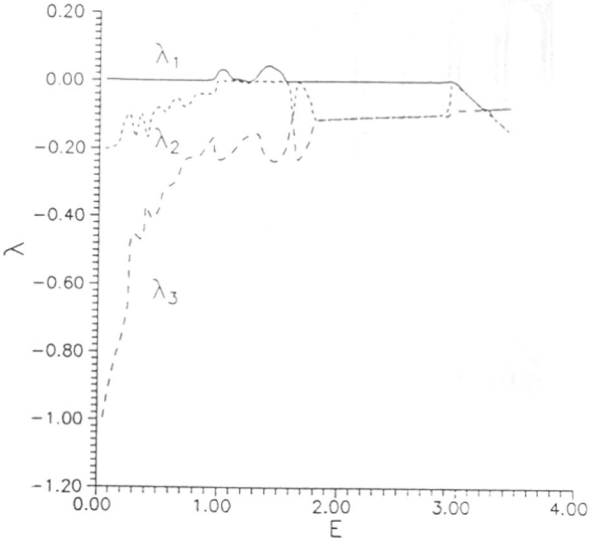

Fig 2.Converged values of the Lyapunov exponents $\lambda_1, \lambda_2, \lambda_3$ *versus* E

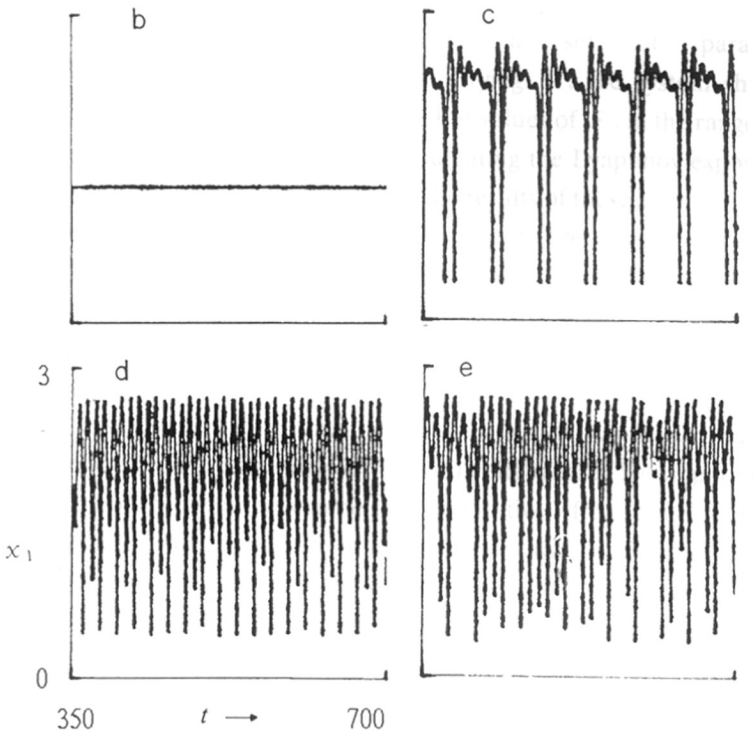

Fig. 2b Temporal behaviour of x_1 for varying $E = 3.0, 1.2, 1.52, 1.42$ (plots b-e, respectively drawn on identical scales).

be explained in terms of information generation in the system and the fractal dimension of the strange attractor. The results obtained in this chapter will form the ground work for the next chapter in which the problem of synchronization and other effects of coupling nonlinear dynamics will be undertaken.

On solving the eqs. (9-11) for a set of parameter values $B = 0.35$, $A = 4.0$, $G = 0.1$, $F = 0.2$, but with varying E, the system shows a range of dynamics from simple stable solutions to chaos. For values of E, in the range of $0.05 - 3.5$ we have obtained the nature of solutions by evaluating the Lyapunov exponents employing the framework outlined before. Fig2a presents the results of these simulations and shows the converged values of the Lyapunov exponents λ_1, λ_2, λ_3, as the parameter E varies. For a value of $E = 3.0$, the system is drawn towards a stable fixed-point (fig. 2b) with $\lambda_1 = -0.0124$ (fig. 2a). Choosing a lower value of $E = 1.2$, yields the case where $\lambda_1 = -0.0000405 \sim 0.0$, indicating the presence of a periodic solution, and the temporal behavior curve clearly shows the dynamics to be multipeak periodic (fig. 2c). For intermediate values of $E = 1.52$, and $E = 1.42$, the system is chaotic since positive values of $\lambda_1 = 0.0136$, and 0.0416, respectively, are obtained (fig. 2a) with $\lambda_2 = 0.0$, in either case. The apparent differences in the chaotic nature of the dynamics can be seen qualitatively from the concentration profiles (figs. 2d,2e). Quantitatively a measure of chaos present can be obtained by calculating the Lyapunov dimension (D_L) for both these cases by eq. (6). They have been found to be $D_L = 2.065$, for $E = 1.52$, and $D_L = 2.185$, for $E = 1.42$, indicating the latter case to be more chaotic. The objective in characterizing the solution behavior in the reported fashion has been to identify cases for studying the properties of coupled systems which forms the theme of the next chapter.

4.8 Interpretation in terms of Information Theory

In terms of information theory we can say that a strange attractor is a generator of information. Liapunov exponents measure the rate at which the system processes or destroys information. L.E. are expressed in terms of bits of information/s or bits/orbit for a continuous system and bit/iteration for a discrete system. In the present study for the parameter $E = 1.42$, the largest L.E. is $\lambda_1 = .0416$ bits/s. Suppose an initial condition was specified with an accuracy of 1 bit, the future behaviour can not be predicted after about 24s (1bit/.0416 bits/s) or about 24 orbits. After 24 orbits a small initial uncertainty will essentially cover the entire attractor, reflecting 1bit of information that can be gained from an initial measurement of the system. This new information results from our inability to specify the state of the system except to say that it is somewhere in the attractor. The asymptotic decay of a perturbation to the attractor

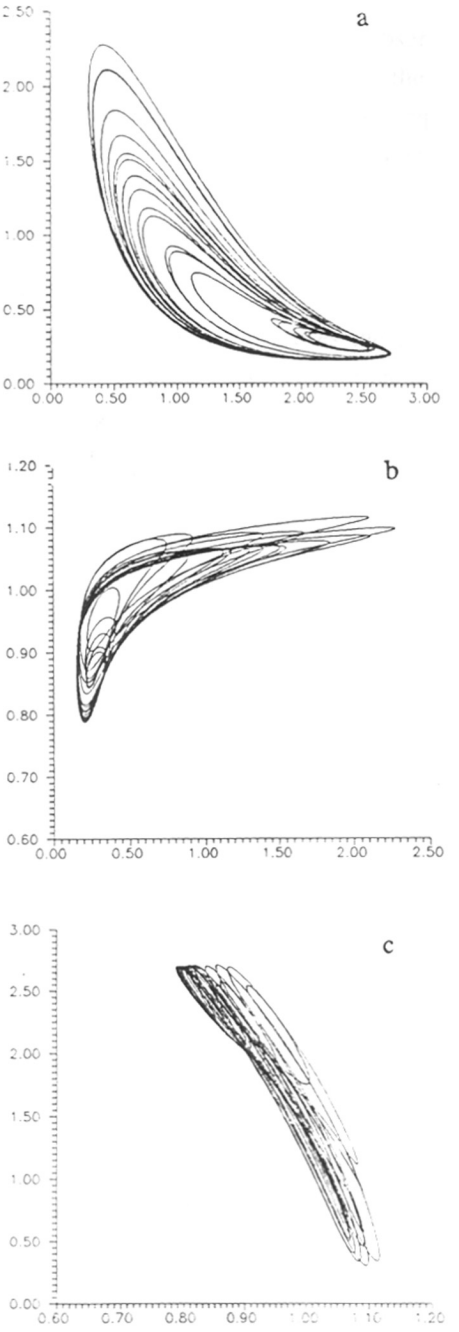

Figure 3 Two dimensional projection of strange attractor for the Selkov model in various planes corresponding to $E = 1.42$ (a) x_2 versus x_1 (b) x_3 versus x_2 (c) x_1 versus x_3

is dictated by the least negative L.E. value. An observer at t=0, needed less information to characterize the two initial closeby conditions. As the time elapses the observer needs more no. of bits to characterize the separated orbits. A comparison with the limit cycle case reveals opposite situation. In the limit cycle case two distinguishable initial conditions become indistinguishable after initial transients have subsided. Thus the information generation in the limit cycle case is zero. In the steady state, information generation is negative.

4.9 Conclusion

To sum up, the present chapter introduces the idea of chaotic dynamics, its origin and significance. Methods to quantify chaotic dynamics are also studied. The glycolytic model as given by Sel'kov is taken as representative case. Parameters corresponding to various dynamic modes are isolated, which will form the groundwork for the next chapter.

4.10 References

1. E.N. Lorentz, J. Atmos. Sci. 20 (1963) 130.
2. (a) C. Sparrow, *The Lorentz Equations, Bifurcations, Chaos and Strange Attractors*, Appl. Math. Sci.41 (1982) Springer-Verlag.
   (b) Hao Bai-Lin (1984) *Chaos,* World Scientific.
3. John Guckenheimer and Philips Holmes, *Nonlinear oscillations, Dynamical Systems and Bifurcations and Vector Fields*, Appl. Math. Sci. 42 (1983) Springer -Verlag.
4. A. J. Lichtenberg and M. A. Lieberman, *Regular and Stochastic Motion*, Appl. Math. Sci. 38 (1983) Springer-Verlag.
5. Ruelle David and Floris Takens, Commun. Math. Phys. 20 (1971) 167.
6. Tien-Yien Li and James A. Yorke, Amer. Math. Month. 82 (1975) 985.
7. B.B. Mendelbrot, *Fractals: Form, Chance, Dimension* (1977) Freeman,San Francisco
8. Per Bak, Chao Tang and Kurt Wiesenfeld, Phy. Rev. Lett. 59 (1987) 381.
9. G. Nicolis and I. Prigogine, *Self Organization in Nonequilibrium Systems- From Dissipative Structures to order through Fluctuation* (1977), Wiley, new York.
10. H. Poincare, *Les Methods Nouvelles de la Mechanique Celeste,* Gauthier-Villars, 1892, Paris.
11. (a) I. Shimada and T. Nagashima, Prog. Theor. Phys., 61 (1979) 1605.
    (b) I. Goldhirsch, P.L. Sulem and S.A. Orszag, Physica 27D (1987) 311.
12. T.C. Halsey, M.H. Jensen, L.P. Kadanoff, I. Procaccia and B.I. Shaiman, Phys. Rev. A 33 (1986) 1141.
13. Hirokazu Fujisaka, Prog. Theor. Phys. 71 No.3 (1984) 513.
14. J.L. Kaplan and J.A. Yorke, Chaotic behaviour of multi-dimensional difference equations, 'in Func. Diff. Eq. and Analysis of Fixed points', Ed. H.O. Peitgen and H.O. Walther, in Lect. Notes in Math., No. 730, Springer-Verlag, pp204.
15. (a) J.P. Eckman and D. Ruelle, Rev. Mod. Phys. 57 (1985) 617.
    (b) R. Shaw, Z. Naturforsch. 36a (1981) 80.
16. M.J. Feigenbaum, J. Stat. Phys. 19 (1978) 25.
17. B.A. Huberman and J. Rudnick, Phy. Rev. Lett. 45 (1980) 154.

18. (a)P.E. Kloeden and A. I. Mees Bull. Math. Biol. 47,(1985) 697.
(b)L.F. Olsen and H. Degn, Quart. Rev. Biophys. 18, (1985) 165.
(c) O. Decroly and A. Goldbeter,Proc. Natl. Acad. Sci. 79, (1982) 6917
(d)J. L. Martiel and A. Goldbeter, Nature, 313 (1985) 390.
(e)T. R. Chay, Physica 16D (1985) 233.
(f)T. R. Chay and J. Rinzel, Biophys. J. 47 (1985) 357.

19. (a) A. Babloyantz and A. Destexhe, Proc. Natl. Acad. Sci. 83 (1986) 3513.
(b) A. V. Holden, W. Winlow and P. G. Haydon, Biol. Cybern. 43 (1982) 169.

20. (a)W. M. Schaffer and M. Kot, Bioscience 35 (1985) 342.
(b) R. May. Nature 261 (1976) 459.

21. Edward Ott, Celso Gregory and J.A. Yorke, Phy. Rev. lett. 64 (1990) 1196.

22. (a)E.E. Sel'kov, Euro. J. Biochem. 4, (1968) 79.
(b) Th. Schulmeister and E.E. Selkov, Stud. Biophys. 65,(1977) 121.

23. Th. Schulmeister, Stud. Biophys. 72 (1978) 205.

CHAPTER V

EFFECTS OF COUPLING NONLINEAR SYSTEMS WITH COMPLEX DYNAMICS

Dynamic behavior of coupled cells, each of which is exhibiting a complex pattern, has been studied as a function of a coupling parameter for a simple model system. Coupling of cells with different dynamics for different cases show a generalized feature, namely, presence of a hyperchaotic regime at low coupling strengths followed by a periodic window at intermediate values followed by synchronization in a chaotic state. The interesting observation of complete synchronization of individual cells even when the coupled dynamics shows chaos is of considerable significance.

5.1 Introduction

Networks of coupled cells with mutual transport of material and energy between them are often used to construct mathematical models for describing physically observed phenomena in physical, chemical and biological systems[1-5]. For example, in biological processes, a linking mechanism among living cells and tissues, can explain morphogenetic, circadian and other biorhythmic system behavior[4]. In other branches of science and engineering, these simple compartmental models are often invoked to describe distributed systems with simultaneous reaction and diffusion. In view of its simplicity, the use of models which allow well-mixed cells to be coupled is convenient to use both in experimental programmes as well as from a conceptual viewpoint for theoretical development[5].

An individual cell whose dynamics follows a nonlinear mechanism can exhibit *a plethora* of dynamic features like simple and multi-peak periodic, intermittency and chaos. In the last chapter this behaviour for a single cell was studied. Indeed, the study of coupled oscillatory cells has served a useful purpose in understanding pattern formations, turbulence, synchronization and entrainment in systems. In asymptotic regimes, for the cases when the cells are weakly coupled, simple perturbation treatments can describe the dynamics quite effectively[7]. Moreover, the output from an entire coupled network may be entrained into a simple oscillator although local phase locking of the individual oscillators need not take place. Synchronization of multi-peak periodic processes with different natural frequencies into that of a common frequency is likely to have important implications in the self-organisation of natural processes.

Dynamic studies of coupled systems, have been generally restricted to analyzing the effects of interactions among limit cycle type oscillators and the solutions have shown the presence of complex features even when the individual oscillators are simple. However, as brought out earlier the individual cells can themselves exhibit multi-peak periodic or chaotic dynamics and previous studies have shown that their presence is not an uncommon system feature. Therefore, it is equally likely that situations could arise wherein individual units exhibiting complex dynamics, albeit, qualitatively different are coupled, and a study of its features forms an interesting problem. Present chapter therefore focuses attention on analyzing the effects of coupling systems with varying types of complex dynamics in its subunits and attempts to do so by analyzing a relevant system, namely, the Sel'kov model[8], which describes the behavior of glycolytic systems. The results obtained do seem to indicate that nonlinear systems of this type can exhibit a wide range of behavioral patterns ranging from simple periodic oscillations on one end of the scale to hyperchaos on the other. Furthermore, for combinations of system

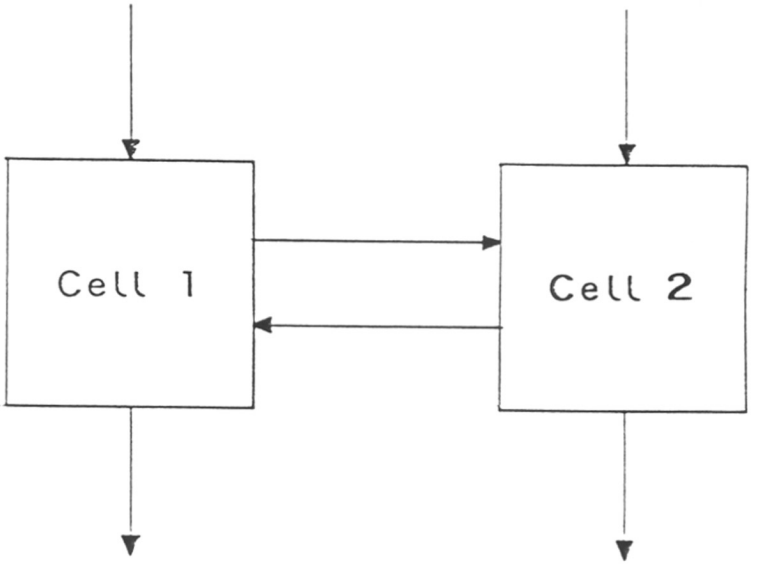

Figure 1 Schematic of Coupled Cells Configuration

parameter values it is shown that there exists a possibility of synchronization taking place among the individual cells even when the long term coupled dynamics of the system clearly show the presence of chaos.

5.2 Model

A living cell can effectively communicate with its neighbours. Such a communication has its role in normal as well as pathological conditions. Gap junctions are specialized structures responsible for diffusive exchange of low molecular weight molecules between cells (intercellular communication). There is increasing evidence that the interaction strength of cells in a tissue can change during ontogenetic development and that this change may result from active regulation of gap junctional structures. Models have been proposed embodying this principle of a regulated diffusional interaction as possible pattern forming systems[4b].

The background necessary for analyzing the complex dynamics of coupled nonlinear system was discussed in the last chapter. For present study a modified version of the Sel'kov model which includes a mechanism for reversible deposition of substrate x_1 into an inactive form x_3 is utilized[8,9]. The governing equations for this process written in the standard form are:

$$\frac{dx_1}{dt} = 1 - Bx_1 - x_1x_2^2 - Ex_1x_2 + x_3 \qquad (1)$$

$$\frac{dx_2}{dt} = A(x_1x_2^2 - x_2 + G) \qquad (2)$$

$$\frac{dx_3}{dt} = F(Ex_1x_2 - x_3) \qquad (3)$$

For simplicity in analysis we consider a skeletal model of two cells with the dynamics in eqs. (1-3) to be coupled by introducing an exchange mechanism between them. Figure 1 shows the schematic of coupled cells. Physically there are a number of known pathways by which species can travel from one cell to another such as through gap junctions, channels, gates, pumps or receptor activated mechanisms. Denoting the dependent variables (x_1 , x_2 , x_3 ,) for the cell 1 to be $x_{1,1}$, $x_{2,1}$, $x_{3,1}$, and cell 2 to be $x_{1,2}$, $x_{2,2}$, $x_{3,2}$, the set of equations describing the coupled model may be written as:

Cell 1

$$\frac{dx_{1,1}}{dt} = 1 - Bx_{1,1} - x_{1,1}x_{2,1}^2 - E_1 x_{1,1}x_{2,1} + x_{3,1} + D(x_{1,2} - x_{1,1}) \qquad (4)$$

$$\frac{dx_{2,1}}{dt} = A(x_{1,1}x_{2,1}^2 - x_{2,1} + G) + D(x_{2,2} - x_{2,1}) \qquad (5)$$

$$\frac{dx_{3,1}}{dt} = F(E_1 x_{1,1}x_{2,1} - x_{3,1}) + D(x_{3,2} - x_{3,1}) \qquad (6)$$

Cell 2

$$\frac{dx_{1,2}}{dt} = 1 - Bx_{1,2} - x_{1,2}x_{2,1}^2 - E_2 x_{1,2}x_{2,2} + x_{3,2} + D(x_{1,1} - x_{1,2}) \qquad (7)$$

$$\frac{dx_{2,2}}{dt} = A(x_{1,2}x_{2,2}^2 - x_{2,2} + G) + D(x_{2,1} - x_{2,2}) \qquad (8)$$

$$\frac{dx_{3,2}}{dt} = F(E_2 x_{1,2}x_{2,2} - x_{3,2}) + D(x_{3,1} - x_{3,2}) \qquad (9)$$

where the exchange coefficient D has been assigned equal values for all the steps. The formulation of eqs. (4-9) assumes that the flux of the dependent variables from one cell to another is proportional to the concentration difference that exists between. This suggests that in the limiting case of both the cells behaving identically in all respects this potential vanishes. Note that to facilitate the consideration of the two cells with differing dynamics *via* the results obtained from the uncoupled system (Chapter 4), we delineate the parameter E, by E_1, and E_2, in eqs. (4-9) for the cells 1 and 2. The solution to eqs. (4-9) can be obtained by solving them for a set of specified initial conditions $x_{i,1}|_{t=0}$, $x_{i,2}|_{t=0}$, $i = 1,2,3$.

5.3 Results and Discussion

The effects of coupling were studied by specifying appropriately the initial conditions and parameter values for each cell corresponding to cases of complex dynamics. System behaviour was characterized in terms of Liapunov exponents[10,11]. The results on solving the sets of eqs. (4-9) for the following cases, namely,

1) multi-peak periodic ($E_1 = 1.2$) cell with a chaotic ($E_2 = 1.52$) cell,

2) chaotic conditions governed by the same attractor in both cells ($E_1 = E_2 = 1.52$) but with different initial conditions, and,

3) chaotic conditions in each cell governed by two distinct attractors $E_1 = 1.42$ and $E_2 = 1.52$,

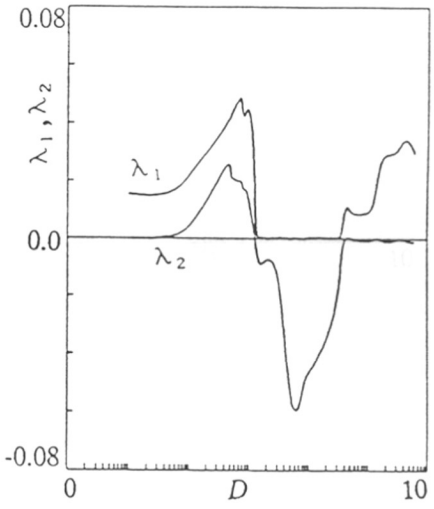

Fig.2. Plot of the two largest Lyapunov exponents λ_1, λ_2, *versus* exchange coefficient D for Case 1.

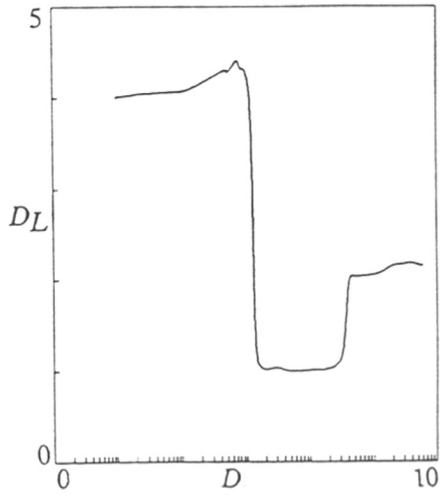

Fig.3. Plot of the Lyapunov dimension D_L *versus* exchange coefficient D for Case 1.

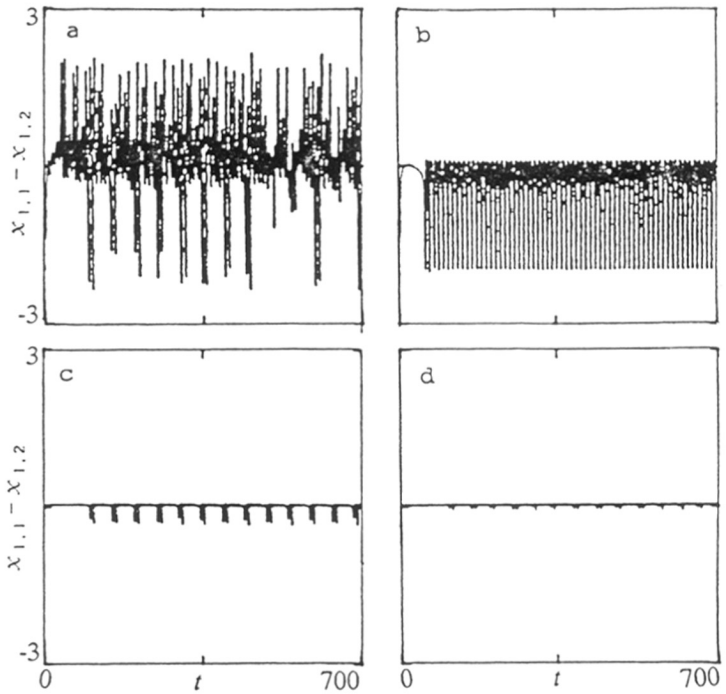

Fig.4. Temporal behaviour of the concentration difference between the coupled cells ($x_{1,1} - x_{1,2}$) for varying values of exchange coefficient $D = 0.001, 0.05, 1.0, 2.0$, (plots a-d, respectively, drawn on identical scales)

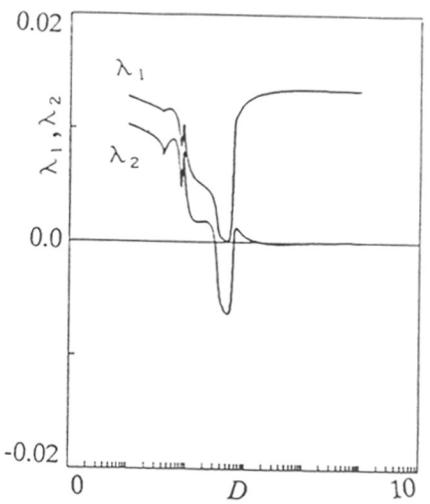

Fig.5. Plot of the two largest Lyapunov exponents λ_1 , λ_2 , *versus* exchange coefficient D for Case 2.

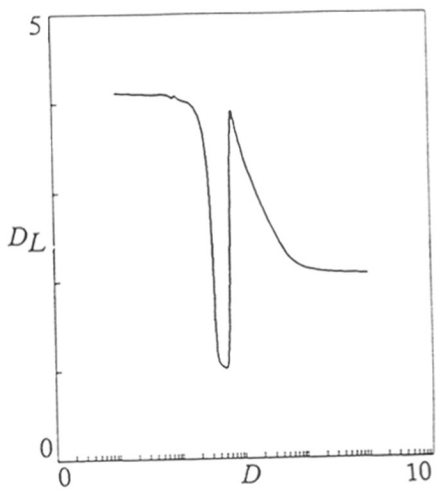

Fig.6. Plot of the Lyapunov dimension D_L *versus* exchange coefficient D for Case 2.

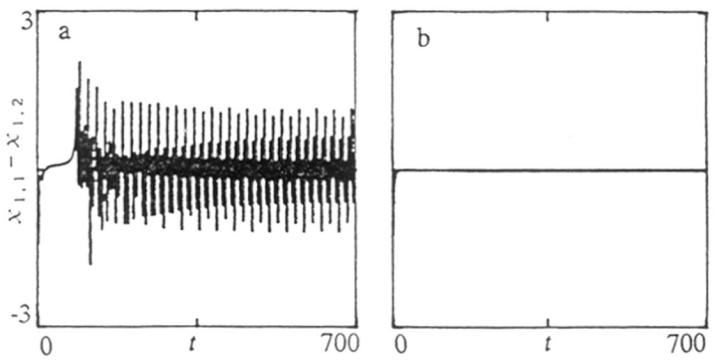

Fig.7. Temporal behaviour of the concentration difference between the coupled cells ($x_{1,1} - x_{1,2}$) for varying values of exchange coefficient $D = 0.005, 0.1$ (plots a,b, respectively, drawn on identical scales)

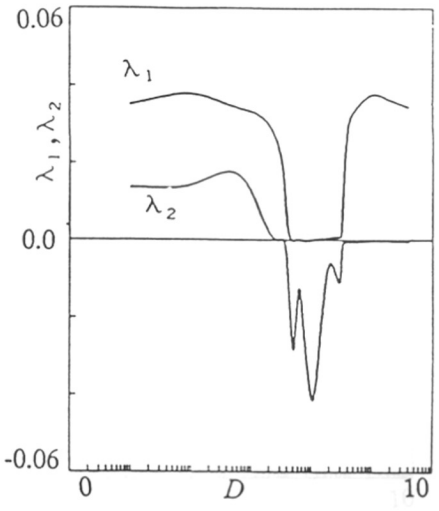

Fig.8. Plot of the two largest Lyapunov exponents λ_1 , λ_2 , *versus* exchange coefficient D for Case 3.

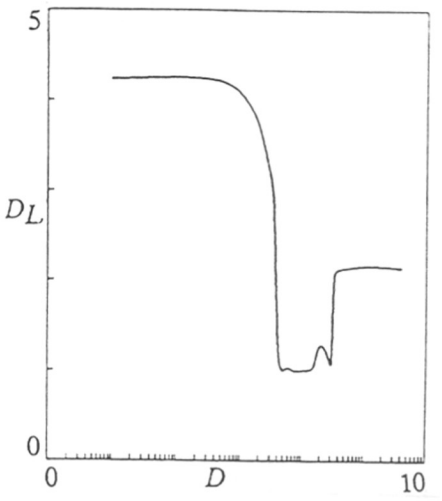

Fig.9. Plot of the Lyapunov dimension D_L *versus* exchange coefficient D for Case 3.

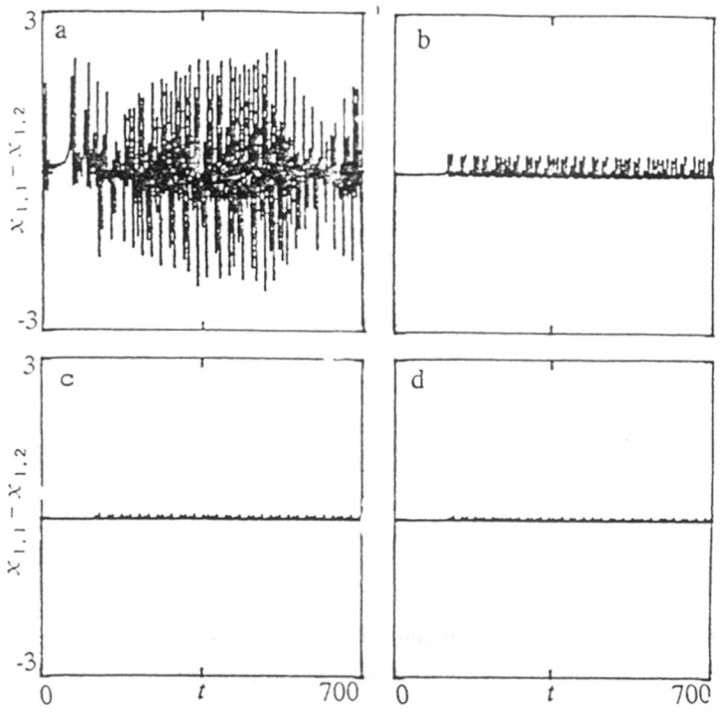

Fig.10. Temporal behaviour of the concentration difference between the coupled cells $(x_{1,1} - x_{1,2})$ for varying values of exchange coefficient $D = 0.005, 0.5, 1.1, 1.2$, (plots a-d, respectively, drawn on identical scales)

are discussed below.

Case 1

The results of simulation, by coupling cells with $E_1 = 1.2$ and, $E_2 = 1.52$ are presented in figs. 2,3. Fig. 2 shows the variation in the two largest Liapunov exponents (λ_1 , λ_2), as a function of the coupling strength (D) which has been varied by orders of magnitude. For low values of $D < 0.012$ we observe that the coupled system is hyperchaotic with both λ_1 , $\lambda_2 > 0$ and $\lambda_3 = 0$ (not shown). For a small increase in the value of D to 0.013 a sharp transition to periodic behavior is seen. The system is then governed by periodicity over a parametric window of coupling strength D. Subsequently for higher values of $D = 0.35$ the system undergoes a fresh transition to a chaotic state with $\lambda_1 > 0$, $\lambda_2 \sim 0$. The changes in the dimensionality of the system as the transitions take place is brought out in fig. 3 where the Liapunov dimension[12], D_L is plotted against D. The calculation of D_L also takes into account all the significant exponents other than the positive ones. At low coupling values of D , corresponding to the hyperchaotic regime the coupled system takes the dimensionality in the range of $4 - 4.5$ which diminishes to 1 in the periodic window and subsequently rises qualitatively to a dimensionality corresponding to those of uncoupled system (in the range of $2. - 2.2$) for higher D values.

Figs. 4a-4d show the direction and magnitude of the concentration differences ($(x_{1,1} - x_{1,2})$) between the coupled cells as a function of time for chosen values of D in increasing magnitude. The values of D depicted in this figure cover situations in the hyperchaotic region, $D = 0.001$, (fig. 4a), periodic window $D = 0.05$, (fig. 4b) and chaos $D = 1.0$, 2.0 , (figs. 4c,4d). The figures clearly reveal the chaotic nature of the flux in the hyperchaos region and the presence of periodic reversals in the periodic window. The plots of the concentration differences at higher values of D are seen to progressively attain values of zero with time indicating that the two cells are behaving in nearly identical fashion. For higher values of D than those presented in these plots complete synchronization can be achieved. An interesting feature of the results for the other two cases discussed below has been that the nature of the transition sequence and also the system behavior is seen to follow the above pattern. A typical time profile wherein complete synchronization takes place is therefore shown as part of the studies for Case 2 without any loss in generality.

Case 2

The coupling of a chaotic cell with another chaotic cell operating under the influence of the same system attractor (i.e., identical parameter space for both the cells) has been studied by allowing the initial conditions for solving eqs. (4-9) to be different. Thus, for Cell 1 we allow the initial conditions at $t = 0.0$ to be

$x_{1,1} = 0.5468$, $x_{2,1} = 1.3039$, $x_{3,1} = 0.02$, while for Cell 2 we let $x_{1,2} = 1.5468$, $x_{2,2} = 0.3039$, $x_{3,2} = 1.02$. Similar to fig. 2 the variation in the significant positive Liapunov exponents (λ_1, λ_2) for varying D, are shown in fig. 5. A comparative assessment of fig. 5 with fig. 2 shows that the coupled system once again qualitatively goes through a transition from hyperchaos to periodic to chaos. A significant departure from the previous case is that the values of D where periodicity occurs has been considerably reduced ($0.0035 \leq D \leq 0.006$) in the present case. The effects of this reduced parametric window in D is seen to induce a relaxation regime, whereby, the system passes through a hyperchaotic region $0.0065 < D \leq 0.007$ before settling down to chaotic regime where $\lambda_2 = 0.0$. The variation in the Liapunov dimension for increasing D is shown in fig. 6 where the varying dimensionality of the system further qualifies the observed transition sequence. It may be noted that for high values of D the system approaches an asymptotic value for its dimensionality $D_L \sim = 2.1$. In figs. 7a,7b the concentration difference profiles for two values of D, namely, $D = 0.005$ and $D = 0.1$ corresponding to a value of D lying within the periodic window and in the asymptotic region of dimensionality are shown. Fig. 7a shows the nature of the concentration difference to be multi-peak periodic while fig. 7b clearly shows complete synchronization of both the cells even though the coupled cells are chaotic (indicated by the positive value of the Lyapunov exponent λ_1).

Case 3

Analyzing the system on coupling two chaotic cells each governed by two different attractors, i.e., by assuming Cell 1 to be associated with a value of $E = 1.42$ while Cell 2 has $E = 1.52$ shows the transitions of the system for varying D to be in the pattern hyperchaos to periodic to chaos once again (see, fig. 8). The dimensionality in the hyperchaotic region (fig.9) is seen to fall down sharply from $D_L = 4.24$ to 1.0 for a small variation in D. However, the presence of a wider periodic window in this case when compared to the earlier one allows for a smoother transition from periodic to chaotic regime. The dimensionality of the system at higher values of D reaches an asymptotic value $D = 2.14$, comparable to the Liapunov dimensions of the uncoupled attractors. Typical deviation profiles in the concentrations between the two cells for $D = 0.005, 0.5, 1.1, 1.2$ are shown in figs. 10a-10d respectively. The approach to synchronization is clearly seen in these figures.

5.4 CONCLUSION

In summary analysis of the effects of allowing a linear coupling mechanism between the constituent cells of a nonlinear process exhibiting complex dynamics has been studied. The study has shown some unique features that systems of this type can describe. In particular, we note that for three different coupled nonlinear situations the system follows a transition

sequence, hyperchaos → periodicity → chaos, for increasing coupling strength. A detailed analysis with respect to the coupling strength shows that the transitions seem to take place in very sharp coupling parameter regions. Furthermore, we have attempted to show that coupled systems allow for synchronized chaos at high values of the coupling coefficient. The finding can be a useful tool for control and communication between chaotic systems. The result is especially interesting in the wake of studies reported for mappings when the coupling is global or long ranged[1,13,14]. The simple model of two dynamically coupled cells can be looked upon as a long-ranged coupled system, since, every element interacts with every other element. Synchronization is known to be possible for long-range globally coupled maps. The results on synchronization reported here for the continuous system, therefore, seem to corroborate the general result. This situation has to be contrasted when the nature of coupling involved is short-ranged where synchronization seems to be difficult[15,16,17,18].

The results of present work can also related with similar studies reported earlier[19,20] on the nature of chaos → hyperchaos transitions in coupled systems. Although these studies use mappings, the results do seem to share some qualitative features. It may, however, be pointed out that while the above study characterizes the transitions as a function of a chosen system bifurcation parameter, present work analyzed the situation where the extent of communication between the cells is varied.

5.5 References

1. K. Kaneko, Phys. Rev. Lett. 63 (1989) 219.
2. P. Hadley and K. Wiesenfeld, Phys. Rev. Lett. 62 (1989) 1335.
3. I. Schreiber and M. Marek, Physica D 5 (1982) 258.
4. (a) T. Pavlidis, *Biological Oscillators: Their Mathematical Analysis* (Academic Press, New York, 1973) (b) O. Sporns and F.F. Seelig, Biosystems 19 (1986) 83;237.
5. M. Kubicek and M. Marek, Computational methods in bifurcation theory and dissipative structures, Springer Series in Computational Phys., (Springer-Verlag, Berlin, 1983)
6. H. Haken, *Advanced Synergetics* (Springer-Verlag, Berlin, 1983).
7. Y. Kuramoto, *Chemical Oscillations, Waves and Turbulence* (Springer-Verlag, Berlin,1984).
8. Th. Schulmeister , Stud. Biophys. 72 (1978) 205
9. H. Herzel, W. Ebeling and Th. Schulmeister, Z. Naturforsch. 42a (1987) 136.
10. I. Shimada and T. Nagashima, Prog. Theor. Phys. 61 (1979) 1605.
11. I. Goldhirsch, P. L. Sulem and S. A. Orszag, Physica D 27 (1987) 311.
12. J. L. Kaplan and J. A. Yorke, Lecture notes in Math., H. O. Peitgen and H. O. Walther, eds, (Springer-Verlag, Berlin, 1979,204)
13. L. M. Pecora and T. L. Carroll, Phys. Rev. Lett. 64 (1990) 821.
14. K. Kaneko, Physica D 41 (1990) 137.
15. Y. S. Tang, A. I. Mees and L.O. Chua, IEEE Trans. Circuits 30 (1983) 620.
16. K. Kaneko, Prog. Theor. Phys. 72 (1984) 480.
17. F. Kaspar and H. G. Shuster, Phys. Lett. 113A (1986) 451.
18. T. Bohr, G. Grinstein, Yu He and C. Jayaprakash, Phys. Rev. Lett. 58 (1987) 2155.
19. G. Baier and M. Klien, Phys. Lett. A 151 (1990) 281.
20. K. Kaneko, Prog. Theor. Phys. 69(1983) 1427.

CHAPTER VI

CHARACTERIZATION OF A SIMPLE AUTOCATALYTIC NETWORK

In the present chapter example of a simple autocatalytic network is taken from literature and its chaotic behaviour is characterized in terms of Liapunov exponents. Significance of the results obtained is also discussed.

6.1 Introduction

Biological systems are characterized by elaborate catalytic reaction network. These networks have the feature that their dynamics is internally controlled, yet within limits, they tend to be stable against external environmental perturbations. Closed positive feedback loops of catalytic reactions between macromolecules or hypercycles[1a] provide a mechanism whereby each species serves to catalyse self reproduction of its successor in the loop. A class of autocatalytic networks subject to mass constraints are reported in literature which have relevance in imperfect catalytic activity (as seen in case of self splicing RNA[1b], hypercycle theory). The properties of these networks can be described with relatively simple differential equations, such as those derived from hypercycle theory[1a]. Further subject to one step transitions, a system composed of a polyfunctional macromolecule (say a polyfunctional enzyme), present in fixed amount together with its ligands (substrates) in a fixed volume, can give rise to variety of rich dynamical phenomena[2a] .

In the present chapter example of a simple autocatalytic network is taken from literature[3] and its chaotic behaviour is characterized in terms of Liapunov exponents. Significance of the results obtained is also discussed.

6.2 Model

The reaction scheme discussed in this chapter includes four 'imperfect catalysts', X's and two cofactors Y's as follows

$$Y_1 + X_1 + X_2 \dashrightarrow 2X_2$$

$$X_2 + X_3 \dashrightarrow 2X_3 + Y_1$$

$$Y_2 + X_3 + X_4 \dashrightarrow 2X_4$$

$$X_4 + X_1 \dashrightarrow 2X_1 + Y_2$$

The underlying differential equations are derived by application of mass action kinetics, i.e.

$$\frac{dx_1}{dt} = x_1(k_4 x_4 - k_1 y_1 x_2) \quad (1)$$

$$\frac{dx_2}{dt} = x_2(k_1 y_1 x_1 - k_2 x_3) \quad (2)$$

$$\frac{dx_3}{dt} = x_3(k_2 x_2 - k_3 y_2 x_4) \quad (3)$$

$$\frac{dx_4}{dt} = x_4(k_3 y_2 x_3 - k_4 x_1) \quad (4)$$

where the k's are kinetic constants, x's and y's refer to the concentration of the catalysts and the cofactors respectively. Since the total concentration of each cofactor is taken to be constant[4], we must have the following conservation conditions.

$$y_1 + x_2 = m_1 = constant$$

$$y_2 + x_4 = m_2 = constant$$

where m_1 and m_2 are the total amount of cofactors, and x_2 x_4 correspond to the concentrations of Y_1 and Y_2 bound to X_1 and X_3 respectively. From equations (1)-(4) we can see that only three variables are truly independent due to conservation of species i.e. $\sum_i dx_i/dt = 0$ and hence $x_1 + x_2 + x_3 + x_4 = constant$. The salient dynamical properties of the system can be shown for a simplified case in which all the k's are assumed to be equal and thus included in the time variable. A further assumption is made that $m_1 = m_2 = m$, so that the system equations become a function of only two parameters, m and c, and the reaction becomes invariant under transformations $x_1 \leftrightarrow x_3$ and $x_2 \leftrightarrow x_4$, Thus system equations become

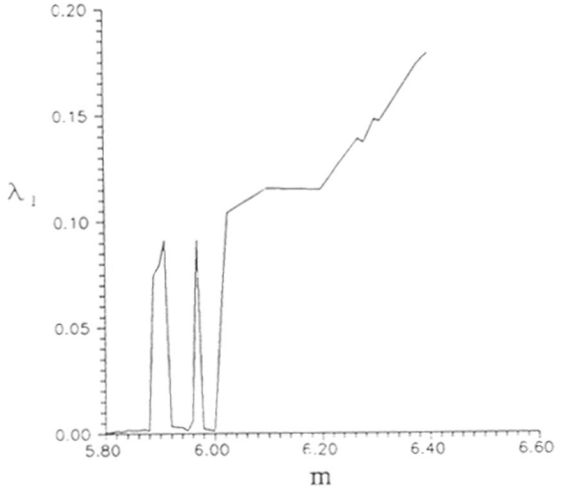

Figure 1 Converged value of largest L.E. λ_1 versus parameter m.

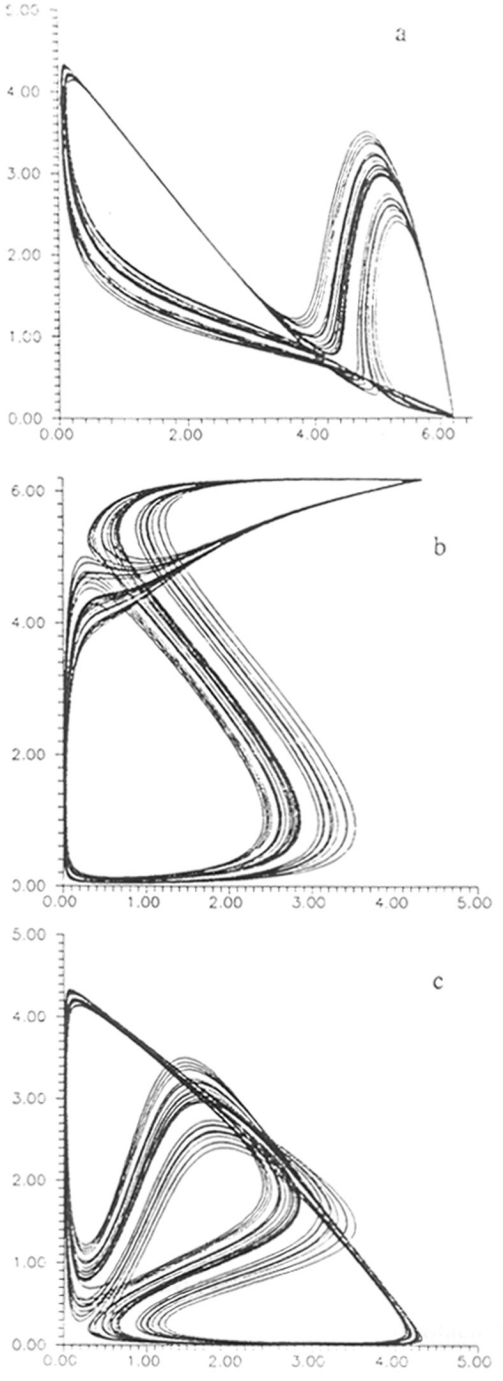

Figure 2 Two dimensional projection of strange attractor for the model in various planes corresponding to $m = 6.2$ (a) x_3 versus x_2 (b) x_2 versus x_1 (c) x_3 versus x_1

$$\frac{dx_1}{dt} = x_1(x_4 - (m - x_2)x_2) \tag{5}$$

$$\frac{dx_2}{dt} = x_2((m - x_2)x_1 - x_3) \tag{6}$$

$$\frac{dx_3}{dt} = x_3(x_2 - (m - x_4)x_4) \tag{7}$$

$$\frac{dx_4}{dt} = x_4((m - x_4)x_3 - x_1) \tag{8}$$

As discussed in the Mori and Cera[3],the Hopf bifurcation occurs at m= 5.444948. As the values of parameter m is increased two stable limit cycles coalesce into a homoclinic orbit involving a saddle point. The orbit then evolves toward a unique, stable orbit which, beyond a critical value of m, is destabilized to give an aperiodic regime whereby formation of a strange attractor is observed. In the present work the system behaviour will be characterized in terms of Liapunov exponents of the system.

6.3 Results and discussion

Equations (5)-(8) were taken to determine the converged values of Liapunov exponents. Figure 1 depicts the converged value of Largest L.E. versus parameter m in the chaotic region. As can be clearly seen positive values of L.E. indicate the exponential divergence of nearby trajectories. Near the onset of chaos one may expect a universal envelope of λ_1

$$\lambda_1(m) \sim |m - m_c|^{\beta}$$

reminiscent of an order parameter near critical point of phase transition[5]. Figure 2 depicts the projection strange attractor of the system in various two dimensional planes. The present analysis raises the question as to the possible role of unbuffering in biochemical systems. Unbuffering a component introduces higher-order non-linearity in differential equations describing the time behaviour of the system. Further studies can be undertaken to investigate what happens if more number of catalysts and cofactors are added in the reaction network.

6.4 References

1. (a) M. Eigen and P. Schuster, *The Hypercycle: A Principle of Natural Self-Organization* (Springer, Berlin, 1979). (b) T.R. Cech and B.L. Bass, Annu. Rev. Biochem. 55(1986) 599.
2. E. Di. Cera, P.E. Philipson and J. Wyman. Proc. Natl. Acad. Sci. USA 85 (1988) 5923.
3. Simone Mori and Enrico Di Cera, Physics Lett A 143 (1990) 369.
4. E. Di. Cera, P.E. Philipson and J. Wyman. Proc. Natl. Acad. Sci. USA 86(1989) 142.
5. B.A. Huberman and J. Rudnick , Phys. Rev. Letts. 45 (1980) 154.

CHAPTER VII

ANALYSIS OF UNSYMMETRICALLY COUPLED SET OF THREE LOGISTIC MAPS

Nonlinear difference equations describing three unsymmetrically coupled logistic maps are analyzed to show existence of multiple basins of attractors and a transition 4P --> 2P --> 4P that proceeds to chaos via period doubling bifurcations. The effects of initial conditions demarcating the basins of attractors are analyzed and show a certain type of symmetry for this unsymmetrically coupled case.

7.1 INTRODUCTION

Nonlinear difference equations have played an important role in understanding of transitions from periodicity to chaos via a sequence of period doubling or subharmonic bifurcations[1-4]. Besides, these equations also provide a projected or stroboscopic representation of a continuous time dynamical system by mapping it on Poincare surface. One dimensional map mimics the dynamics of many component systems of chemical, biological and physical interest[5]. These simple maps, however, can not account for features such as coexistence of attractors which may appear in many realistic cases[6]. Thus in cellular automaton various patterns are known to coexist[7]. In the neural dynamics, multiple stationary states correspond to various memories stored in the system and different memory locations can be addressed by different sets of initial conditions[8].

The most natural generalization of the simple map is to couple two sets of difference equations and in fact such coupling has already been discussed in the literature[9-11]. The introduction of the second competing variable may generate some new pattern that is not possible for the simple uncoupled system. Several studies aiming at understanding the instability and chaotic behavior of such coupled systems are available. The type of coupling envisaged is usually symmetric bilinear (of the type $X_i Y_i$)[10], or the simple linear γX_i, γY_i or $\gamma(X_i - Y_i)$[9, 11]. A case wherein the output of one cell modifies the parametric control of the other and vice versa has also been reported[12]. The studies reveal remarkable differences with respect to the well known sequence of instabilities known for simple 1-d map. In addition, common patterns can be identified for different types of couplings, giving clues to universal behavior.

The studies on coupled maps are numerous, and the models considered use the simplifying feature of binary variables which represent the state of cell. These models are rewritten in terms of dynamic spin problems to establish contact with the extensive investigations reported on spin glass[13]. Two simplifying assumptions, (1) symmetric coupling

and (2) full connectivity i.e. every cell is coupled to every other cell, that are often used in model investigation are however restrictive from the point of view of real situations. The simple case of two cell coupling satisfies these assumptions naturally making it imperative to consider the next simple situation of three coupled cells, if the effects of the coupling other than those due to the assumption stated above are to be investigated.In the present work we shall thus consider coupling between three cells.

To be specific we shall consider three logistic maps that are coupled unsymmetrically. The analysis of three coupled difference equation system, by virtue of its higher dimensionality, is much less transparent than the simple logistic equation or two cell coupled system[14]. Unsymmetric coupling is known to exist in the model of neural networks and corresponds to the observed behavior in real systems[15]. In the situations involving two predators or preys, a three equation model can effectively mimic the dynamics. This model may also be useful to study the interaction of polyatomic molecules with strong IR radiation fields to explain selective multiphoton dissociation[16]. It is expected that heterogeneous couplings among the cells would play an important rolein producing a variety of collective behaviours such as formation of a coordinated pattern as a global order. The system of spin glass where interactions among the spins are heterogeneous can provide a useful example. It is known for instance that the minimum energy state of all individual interactions among spins is inconsistent with the ground state of the system and that the individual interactions mutually compete giving rise to frustration. The competition among the individual interactions modulates the dynamic behaviour of the system in some characteristic ways and one of the interesting problems is to elucidate the variety of dynamic modes in mutually interacting system with heterogeneity. The unsymmetrically coupled system of three logistic maps provides the simplest possible case for this purpose. It should be noted, however, that the system considered here is generic in character and hence no attempts to identify the set of equations with any specific experimental situation are made. The qualitative results,

however,should be generally useful.

7.2 MODEL

The three-unsymmetrically coupled logistic map under study is described as:

$$x_{n+1} = 1 - \lambda_1 x_n^2 + D_1(y_n - x_n) + D'_1(z_n - x_n)$$

$$y_{n+1} = 1 - \lambda_2 y_n^2 + D_2(x_n - y_n) \qquad (1)$$

$$z_{n+1} = 1 - \lambda_3 z_n^2 + D_3(x_n - z_n)$$

The behavior of the set of coupled equations depends on seven parameter values. We have extensively searched the parameter region with a view to identify parameter space where qualitatively different behavior than known for two-cell coupled system can occur. In most instances the behavior corresponds to the type already known except in a few cases where differences can be noticed. In the present letter we shall only point to these differences. To reduce our numerical task, we confine ourselves to a subspace of parameters setting $\lambda_1 = \lambda_2 = \lambda_3$ and $D_1 = D'_1 = D_2 = D_3$. In the event of $D'_1 = 0$ we recover the 2-cell coupled system. Iterations in equation (1) were carried out with initial conditions $x_0 = 0.2, y_0 = 0.3, z_0 = 0.4$ for three values of $D = 0.01, 0.05, 0.1$. The bifurcation diagram is shown in fig. 1 (a, b and c). As can be seen from the figures the bifurcation point shifts toward lower value of λ as the value of parameter D is increased. Thus for $D = 0.01, 0.05, 0.1$ the values of λ for which first bifurcation occurs are 0.74, 0.56 and 0.47 respectively. The corresponding value of λ for the simple logistic equation is 0.75. The figures also show the onset of chaos which occurs at $\lambda = 1.45, 1.4, 1.33$ corresponding to $D = 0.01, 0.05, 0.1$ respectively. The values as expected differ from $\lambda = 1.4011$ corresponding to logistic map. Thus we see that when the interaction among the equations is very weak or strong, the onset of chaos shifts considerably while for intermediate values of coupling the relative change is insignificant. Also for weakly coupled equations the onset of bifurcation does not differ appreciably from the single logistic map. Stated otherwise, the

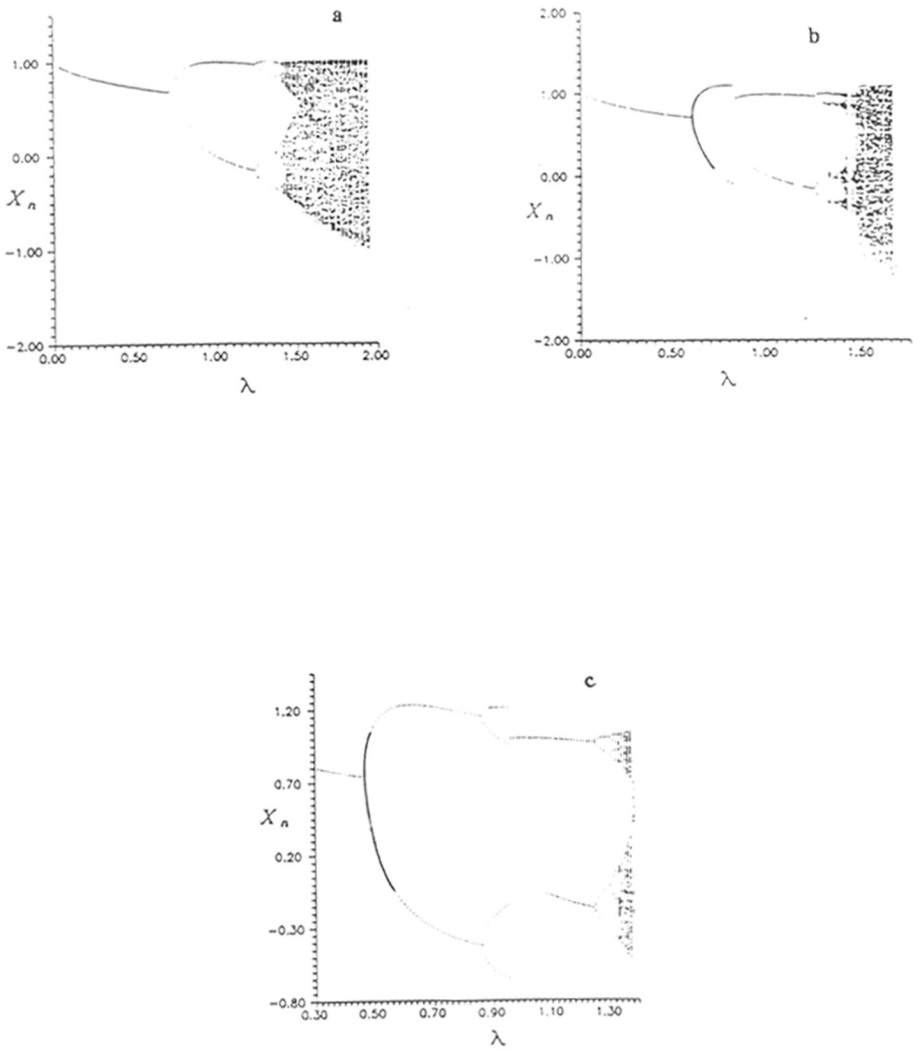

Fig 1. Bifurcation sequence for the variable X_n versus λ (a) $D = 0.01$ (b) $D = 0.05$ and (c)$D = 0.10$.

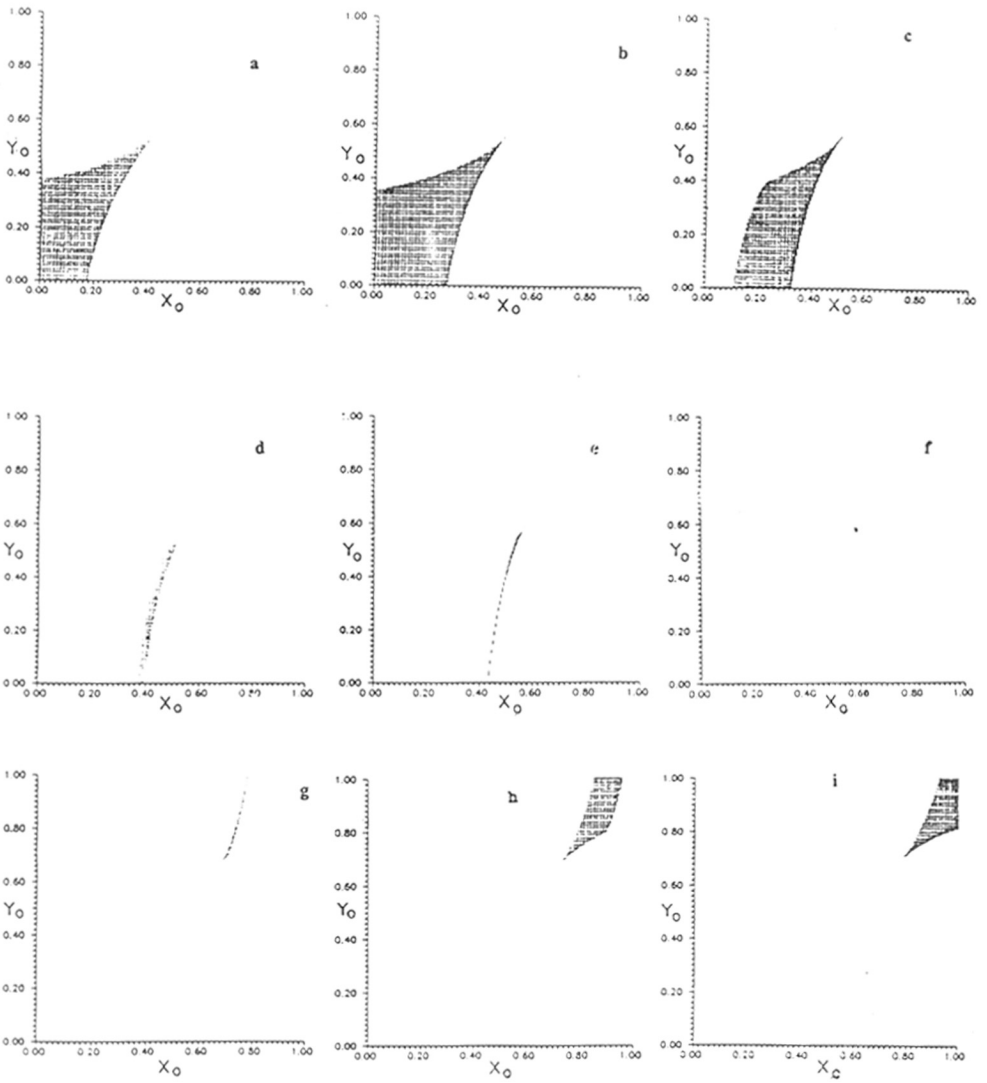

Fig 2.Initial conditions in the $X_0 - Y_0$ plane, which evolve to 2P solutions for a fixed value of the Z_0-coordinate (a) Z_0 = .01 (b) Z_0 = .30 (c) Z_0 = .40 (d) Z_0 = .50 (e) Z_0 = .55 (f) Z_0 = .60 (g) Z_0 = .70 (h) Z_0 = .80 (i) Z_0 = .99. The values of other parameters are, λ = 0.965, D = 0.1.

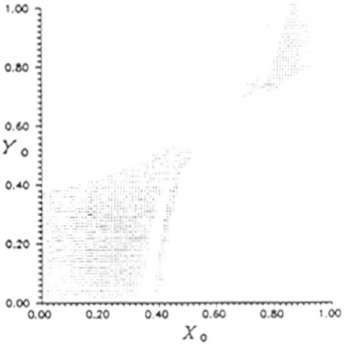

Fig 3. Superimposed view indicating symmetry of initial conditions along the diagonal for the parameter $\lambda = 0.965$ and $D = 0.10$.

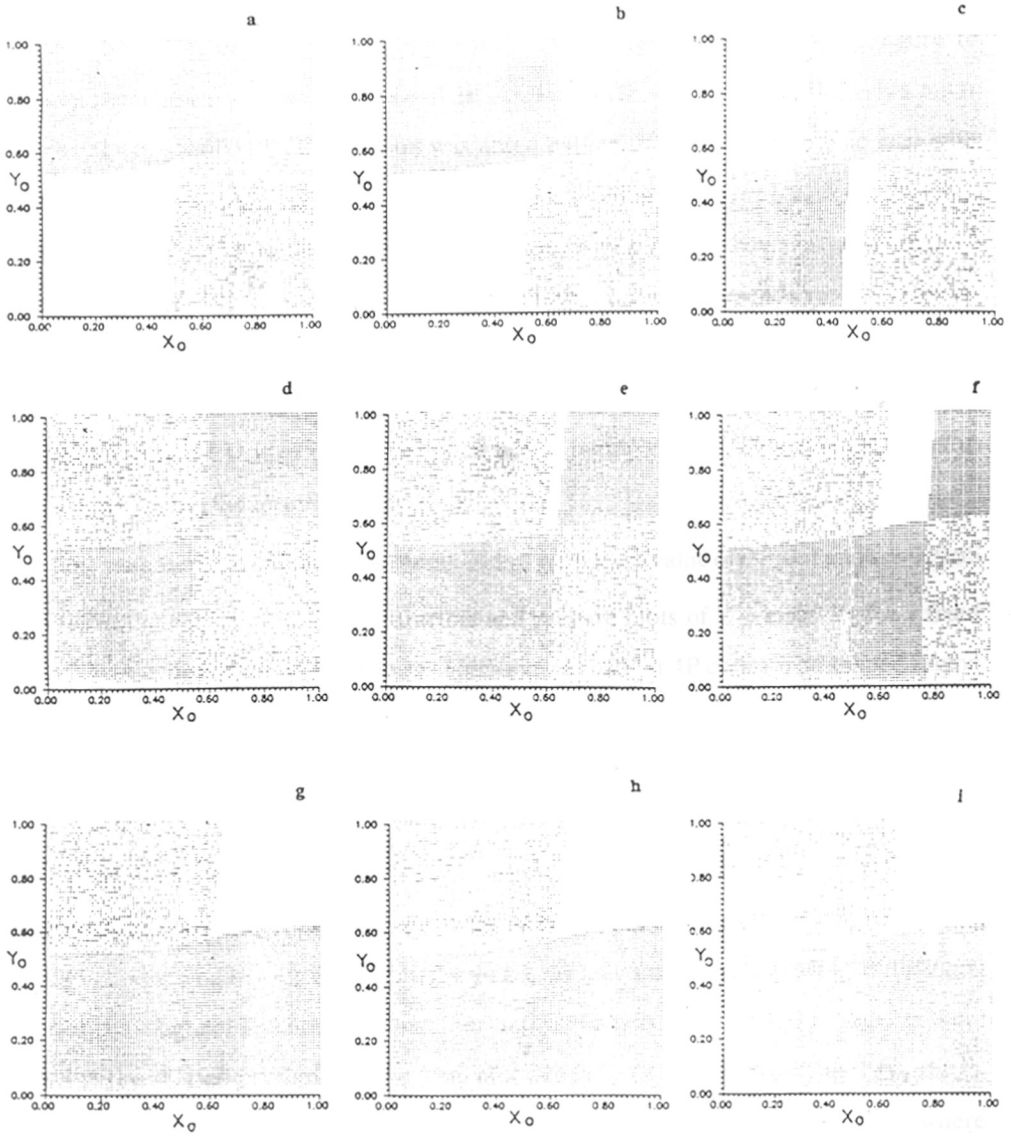

Fig 4. Initial conditions in the $X_0 - Y_0$ plane, which evolve to chaotic solutions for a fixed value of the $Z_\sigma$coordinate (a) $Z_0 = .10$ (b) $Z_0 = .50$ (c) $Z_0 = .55$ (d) $Z_0 = .57$ (e) $Z_0 = .59$ (f) $Z_0 = .61$ (g) $Z_0 = .70$ (h) $Z_0 = .80$ (i) $Z_0 = .90$. The values of other parameters are $\lambda = 1.3$, $D = 0.05$

onset of bifurcation shifts considerably to lower values of λ as the coupling strength increases. On the other hand the onset of chaos shifts to lower or higher values of λ when the coupling becomes very strong or weak respectively. For the case corresponding to $D = 0.1$, figure 1c clearly shows a new transition sequence of 2P --> 4P --> 2P --> 4P. A qualitatively similar behavior of 4P --> 6P --> 4P transition was noted earlier for a coupled logistic map with linear and symmetric coupling [9]. The study reveals coexisting states, the basins of attraction of which depend on the initial conditions and the parameter λ. We have also analyzed the coexistence of such basins of attractors and additionally note their dependence on the value of the coupling strength. For the values of $D = 0.01, 0.05, 0.1$ the corresponding values of λ wherein multiple basins of attractors start appearing are 1.19, 1.05 and 0.908 respectively. Thus as the value of D is increased the point where multiple basins of attraction begin to occur shifts towards the lower value of λ.

For presenting the effects of initial conditions, we select a value of $D = 0.1$ and $\lambda = 0.965$ which lie in the region of multiple attractors and prepare plots of Y_0 versus X_0 for a fixed value of Z_0, marking out the initial points which evolve to 2P or 4P cycles. The shaded region in figure 2 represents the set of points which evolve to 2P solutions. The remaining white portion represents initial conditions which evolve to 4P solutions. This shaded region in the figure shows interesting transition as Z_0 is increased. Thus for higher values of $Z_0 = 0.05, 0.3$ the shaded portion increases in its extent, moving up along the diagonal line as well as along the x-axis while a slight decrease along the y-axis can be noticed. For further increase ($Z_0 = 0.4$) the shaded portion detaches itself from the y-axis, actually shrinks in size while still moving up along the diagonal line and the x-axis. For further increase in Z_0 the shrinkage is faster rendering the shaded portion into the form of a thin strip ($Z_0 = 0.5, 0.55$) that eventually reduces to a point for $Z_0 = 0.6$. Notice the initial conditions that correspond to this case where all coordinates take nearly the same value. For further increase in $Z_0 = 0.7, 0.8, 1.0$, the figure shows an inversion with similar sequence repeating in reverse order. All these figures

can be superimposed on each other showing considerable region of overlap with respect to initial conditions which will lead to 2P solutions. The entire region lie along the diagonal and exhibit some type of symmetry (figure 3).

Similar analysis has been repeated for another set of parameter values $\lambda = 1.3$ and $D = 0.05$. Figure 4a shows the plot of initial condition of X_0 and Y_0 for a fixed value of Z_0. The figure clearly demarcates three regions comprising of a dense, rarified and clear white portion. For initial conditions in the clear white region the three coupled cell system evolves to 4P solution while the dots correspond to initial conditions that lead to chaotic behavior of the system. As expected these regions vary in their extent depending on the initial values of Z_0. The relative variations are however insignificant for values of $Z_0 < 0.5$. Beyond this value of Z_0 the clear white region begins to diminish and rarified region increases. The white region is actually replaced by a denser region and part of the original dense region becomes rarified creating a cross shaped boundary. One can actually notice a thin strip of clear white region for $Z_0 = 0.55$ which is completely lost as for example when $Z_0 = 0.58$. Increasing Z_0 beyond causes reemergence of a clear white region strip; however the sequence now appears inverted $Z_0 = 0.59$. Simultaneously the lower tier of the dense region shows building up tendency ($Z_0 = 0.6, 0.61$) until at $Z_0 = 0.7$ the clear white region swaps the entire denser region in the upper tier. The three regions noticed for lower values of Z_0 now reappear with their positions inverted ($Z_0 = 0.7, 0.8, 0.9$). The simple case of three coupled logistic maps with unsymmetric couplings again exhibit some kind of symmetry with regard to initial conditions that specify multiple basins of attractors.

7.3 Conclusions

To summarize, present chapter analyses a set of equations that describes three unsymmetrically coupled logistic maps and show the existence of multiple basins of attractors and a transition 4P --> 2P --> 4P. For certain values of coupling strength, the effects of changing initial conditions are analyzed and show a certain type of symmetry for this

unsymmetrically coupled case. Model equations describing logistic maps or their coupling are often used to understand and explain behavioral features of many physical, chemical and biological systems. These simple equations, while provide qualitative explanation for many observed features, are unable to explain certain other features. The case treated here may help to further our understanding of such systems.

7.4 REFERENCES

[1] M.J. Feigenbaum, J. Stat. Phys. 19, (1978) 25; 21, (1979) 669; Phys. Lett. 74a, (1979) 375.

[2] P. Collet and J.P. Eckman, Iterated Maps on the Interval as Dynamical systems(Birkhauser, Basel, 1980).

[3] E. Ott, Rev. Mod. Phys., 53, (1981) 655.

[4] R.M. May, Nature 261, (1976) 459, J.R. Beddington, C.A. Free and J.H. Lawton, Nature, 255 (1975) 58.

[5] P. Cvitanovic ed. Universality in Chaos (Hilger, Bristol,1984); J. L. Hudson and J.C. Mankin, J. Chem. Phy. 74, 6171 (1981); Y. Kuramoto, in Springer Series in Synergetics, Vol. 19, Chemical Oscillations, Waves and Turbulence.(Springer 1984) pp130.

[6] V. Franceschini, J. Stat. Phys. 22 (1980) 397; F.T. Arecchi, R. Baddi and A. Politi, Phy. Rev. A29 (1984) 1006.

[7] S. Wolfram, Rev. Mod. Phys. 55 (1983) 601.

[8] J.J. Hopfield, Proc. Natl. Acad. Sci. 79 (1982) 2554.

[9] Alessandro Ferretti and Naseem K. Rahman, Chem. Phys. Lett. 140 (1987) 71.

[10] Jian-Min Yuan, Mingwhei Tung, Da Hsuan Feng and Lorenjo M. Narducci, Phys. Rev. A 28 (1983) 1662.

[11] K. Kaneko, Prog. Theor. Phys. 69 (1983) 1427.

[12] Martin P. Paulus, Stephen F. Gass and Arnold J. Mandell, Physica D40 (1989) 135.

[13] Fischer K., Phys. Status Solidi 116 (1983) 357.

[14] Satoshi Omata, Yoko Yamaguchi and Hiroshi Shimizu, Physica D31 (1988) 397.

[15] E. Domany and R. Meir, Europhys. Lett. 2(3) (1986) 175.

[16] N. Bloemberger, Opt. Commun. 15 (1975) 416.

CHAPTER VIII

CONCLUSIONS

The research work in the thesis has been carried out with an objective to explain some of the features observed in nonlinear dynamical systems of general relevance to biology. These features illustrate newer dynamic patterns observed in the field of biology. The models studied involve dynamical systems described by differential as well as difference equations.

Delayed feedback mechanisms occur in many dynamical systems. The effect of delayed feedback on logistic map show that chaotic behaviour can be modulated with introduction of delayed feedback. For intermediate values of parameter α, which quantifies delayed feedback, any kind of periodic or chaotic behaviour is suppressed. For higher values of α system admits period doubling route to chaos. In the second case study, example of cubic autocatalysis occurring in a CSTR is taken. The results show presence of bursting phenomena. Contrary to the belief that very complex models are needed to explain this kind of phenomena, it is observed in case of a very simple model of cubic autocatalysis with the effect of time delay introduced in the system equations. In the irreversible version of cubic autocatalysis in a CSTR, some fraction from the reactor output stream is recycled back into the cell after a delay. This introduces two new parameters in the system viz. time lag τ and fraction recycled λ. Bursting phenomena occurs when the slower large amplitude fundamental oscillations in the CSTR are progressively disturbed by small, parasitic oscillations. The appearance and disappearance of oscillatory bursting has been characterized with respect to fraction recycled and time delays. The study also includes the case where two recycle streams with different time delays are included in the system.

Fractals characterize irregular objects, which are envisaged as deviations from regular integer dimensional objects. These objects are characterized by their fractal dimension, a measure which assumes importance when the texture, roughness, dislocations and inhomogeneities assume a significant proportion such that the idea of a homogeneous object is no more valid. A multi-step reaction is studied on a DLA (Fractal) surface for its selectivity behavior using random walks. Periodic boundary conditions ensured that the simulated system is effectively part of an infinite system. Various methods are tried to decrease the computational time during the Monte-Carlo simulations. To specifically account for the percentage area occupied by active site and the fact that not all collisions will be energetically favored, various probabilities are assigned to each reaction step within physically realistic parameter ranges. The effects of varying probability of reaction steps and rate constants on selectivity behavior have also been studied. Regions have been isolated where maxima and minima of selectivity occur for the system.

Chaotic phenomena is characterized by sensitivity to initial conditions and exponential divergence of nearby trajectories. Liapunov Exponents (LE) are the invariant properties of the underlying attractor which facilitate easy interpretation with respect to stability properties. The LE spectrum of a dynamical system is the signature of its dynamics. Chaotic dynamics is characterized by one positive LE. A hyperchaotic dynamical system is characterized by at least two positive LE. In this study glycolytic model in a living cell as proposed by Selkov is taken as the model system. Parameters corresponding to steady stable state, periodic, complex-periodic and chaotic dynamics are identified. Results have been interpreted in terms of information generation and loss in the system as it evolves. Further extensive investigation has been carried out to know what happens if an array of such cells start influencing each other dynamically. The idea that, two chaotic cells when coupled will synchronize, runs counter to our intuition. However, synchronization is demonstrated in coupled chaotic cells, together with emergence of periodicity in some other parameter values. A universal behavior of

hyperchaotic-> periodic -> chaotic behavior has also been found in coupled cells.

A class of autocatalytic network subject to mass constraints reported in the literature which has relevance in imperfect catalytic activity (as seen in the case of self-splicing RNAs, hypercycle theory). System dynamics is characterized in terms of Liapunov exponents. Further an envelope of largest L.E. versus bifurcation parameter as reported in the literature is reproduced.

Difference equations arise in many contexts in the biology, economics, hydrodynamics and population dynamics. One dimensional mappings of an interval onto itself are simple enough to be accessible to certain analytical tools and are not very time consuming in numerical study. Mappings often provide the clues for understanding chaotic transition in higher dimensional systems. In contrast to 1-d mappings, higher dimensional mappings offer the possibility of multiple stationarity. Starting from different basins of attraction, system settles to different periodic or aperiodic orbits. Example of logistic map is taken for the analysis. In the three coupled cell configuration, we chose the case wherein one cell can communicate with two others. This kind of unsymmetric coupling is reported in the literature for neural networks and spin-glass models. A new bifurcation transition of 4P--> 2P--> 4P is found, that proceeds to chaos via period doubling. The effects of initial conditions demarcating the basins of attractors have also been analyzed and show certain type of symmetry for this unsymmetrically coupled case.

List of Publications

1.	S.S. Tambe, P. Badola and B.D. Kulkarni	Selectivity behaviour of a multi-step reaction on a catalyst modelled as a DLA fractal surface.	Chemical Physics Letters 173 (1990) 67.
2.	Parkash Badola, R. Prasad, V. Ravi Kumar and B.D. Kulkarni	Bursting solutions for Cubic Autocatalysis in a CSTR with Recycle and Time Delay	J. Phys. Chem.95 (1991) 2939.
3.	Parkash Badola, V. Ravi Kumar and B.D. Kulkarni	Effects of coupling nonlinear systems with complex dynamics	Phys. Lett. A 155 (1991) 365.
4.	Parkash Badola and B.D. Kulkarni	Analysis of Unsymmetrically Coupled Set of Three Logistic Maps	Chemical Physics Lett.(in Press)
5.	Parkash Badola and B.D. Kulkarni	A Case of Periodic Parameters	(Under preparation)
6.	Parkash Badola and B.D. Kulkarni	Effects of Random Coupling in a Network of 1-d maps	(Under preparation)